Phys. Lett. B 876 (2026) 140359

Contents lists available at ScienceDirect

Physics Letters B

journal homepage: www.elsevier.com/locate/physletb

Letter

Characterizing the initial state and dynamical evolution in XeXe and PbPb collisions using multiparticle cumulants

The CMS Collaboration [1]

CERN, Geneva, Switzerland

ARTICLE INFO

Editor: Dr. M. Doser

Keywords:
CMS
Heavy ion
Flow
QGP
System size

ABSTRACT

For the first time, correlations among mixed-order moments of two or three flow harmonics —(v_n^k, v_m^l) and (v_n^k, v_m^l, v_p^q), with k, l, and q denoting the respective orders—are measured in xenon–xenon (XeXe) collisions and compared with lead–lead (PbPb) results, providing a novel probe of collective behavior in heavy ion collisions. These measurements compare a nearly spherical, doubly-magic ^{208}Pb nucleus to a triaxially deformed ^{129}Xe nucleus, emphasizing the sensitivity to initial-state geometry fluctuations arising from nuclear deformation. The dependence of these results (v_n, $n = 2, 3, 4$) on the shape and size of the nuclear overlap region is studied. Comparisons between v_2, v_3, and v_4 demonstrate the importance of v_3 and v_4 in exploring the nonlinear hydrodynamic response of the quark-gluon plasma (QGP) to the initial spatial anisotropy. The results constrain initial-state model parameters that influence the evolution of the QGP. The CMS detector was used to collect XeXe and PbPb data at nucleon-nucleon center-of-mass energies of $\sqrt{s_{NN}} = 5.44$ and 5.36 TeV, respectively. Correlations are extracted using multiparticle mixed-harmonic cumulants (up to eight-particle cumulants) with charged particles in the pseudorapidity range $|\eta| < 2.4$ and transverse momentum range $0.5 < p_T < 3$ GeV/c.

1. Introduction

High energy heavy ion collisions at the LHC create a hot and dense state of strongly interacting matter, known as the quark–gluon plasma (QGP) [1,2]. The anisotropic shape of the overlap region between the two colliding nuclei generates pressure gradients that drive a collective anisotropic expansion of the medium. This collective behavior, known as anisotropic flow [3], is quantified through a Fourier decomposition of the single-particle azimuthal distribution of produced particles [4]:

$$\frac{dN}{d\phi} = \frac{1}{2\pi}\left[1 + 2\sum_{n=1}^{\infty} v_n \cos n(\phi - \psi_n)\right], \tag{1}$$

where ϕ is the azimuthal angle of an outgoing particle, ψ_n denotes the nth-harmonic symmetry plane, and v_n is the nth flow harmonic. The coefficients v_2, v_3, and v_4 correspond to elliptic, triangular, and quadrangular flow, respectively. These harmonics carry information about the initial spatial anisotropy and the subsequent medium response.

Event-by-event fluctuations in the positions of nucleons within the colliding nuclei lead to variations in the initial energy density, causing flow harmonics to fluctuate on an event-by-event basis. These fluctuations are studied through higher-order cumulants of the flow coefficients (v_n^k, $k > 1$). While second-order cumulants of a single flow harmonic and two-harmonic correlations are well explored [5,6], they are insensitive to non-Gaussian features of the flow probability distribution [7]. The study of mixed-order cumulants (correlations between different harmonics and orders, v_n^k and v_m^l, with $n \neq m$ and $k \neq l$) provides sensitivity to the nonlinear hydrodynamic response of the QGP. A purely linear response results in v_n scaling linearly with the corresponding initial-state eccentricity ε_n, which quantifies the transverse shape anisotropy of the collision zone immediately after impact [7].

In addition to event-by-event fluctuations in the energy density within each nucleus, the shape of the colliding nuclei, whether spherical or deformed, also influences the initial geometry of the overlap region and, consequently, the observed flow. The doubly magic lead (^{208}Pb) nuclei are nearly spherical [8], whereas xenon (^{129}Xe) nuclei are triaxially deformed [9]. This study therefore probes differences in the initial-state fluctuations arising from event-by-event variations in the nucleon configuration in collisions of nuclei with different shapes. The nuclear shapes are characterized by static ground-state deformation parameters constrained by low-energy nuclear physics measurements [10]. Following the parameterization used in low-energy nuclear structure studies, the nuclear density distribution is described using the Woods–Saxon formula:

$$\rho(r, \theta) = \frac{\rho_0}{1 + \exp[(r - R(\theta))/a_0]}, \tag{2}$$

where r is the radial distance from the center of the nucleus, θ is the polar angle relative to the symmetry axis, ρ_0 is the central density at $r = 0$, and a_0 is the nuclear skin depth. For a deformed nucleus, the

Contact authors: cms-publication-committee-chair@cern.ch.
[1] Authors are listed at the end of this paper.

https://doi.org/10.1016/j.physletb.2026.140359
Received 30 October 2025; Received in revised form 4 March 2026; Accepted 12 March 2026
Available online 16 March 2026

radial term $R(\theta)$ includes angular dependence via spherical harmonics:

$$R(\theta) = R_0\left[1 + \beta_2 Y_{20}(\theta) + \beta_4 Y_{40}(\theta)\right], \quad (3)$$

where R_0 is the mean nuclear radius, β_2 and β_4 are the quadrupole and hexadecapole deformation parameters, respectively, and $Y_{\ell 0}(\theta)$ are the spherical harmonics.

This Letter presents a comprehensive study of multiparticle cumulants involving one, two, and three flow harmonics, including mixed higher-order correlations between different harmonics. The analysis is based on data collected with the CMS detector for XeXe and PbPb collisions at nucleon-nucleon center-of-mass energies of $\sqrt{s_{NN}} = 5.44$ and 5.36 TeV, respectively. The XeXe and PbPb data were recorded in 2017 and 2023, respectively, and correspond to integrated luminosities of 3.42 μb^{-1} [11–13] and 1.92 nb^{-1}. The key goals of this study are: (i) to investigate the effects of nuclear deformation on flow correlations using XeXe and PbPb comparisons, and (ii) to probe the nonlinear hydrodynamic response of the QGP using higher-order moments of v_n. The results are compared to a range of theoretical models to constrain the initial-state geometry and the transport properties of the QGP formed in heavy ion collisions at the LHC. Tabulated results for this analysis can be accessed in the HEPdata record [14].

2. The CMS detector

The CMS detector is centered around a superconducting solenoid with an internal diameter of 6 m, generating a 3.8 T magnetic field [15,16]. Within the solenoid volume reside a silicon pixel and strip tracker, a lead tungstate crystal electromagnetic calorimeter (ECAL), and a brass-and-scintillator hadron calorimeter (HCAL), each composed of a barrel and two endcap sections. Forward calorimeters extend the pseudorapidity (η) coverage of the barrel and endcap detectors. Muons are identified using gas-ionization chambers embedded in the steel flux-return yoke outside the solenoid. The hadron forward (HF) calorimeters, positioned symmetrically 11.2 m from the interaction region, cover the range $3.0 < |\eta| < 5.2$ and also serve as luminosity monitors. These HF calorimeters use steel absorbers and quartz fibers as sensitive material, are azimuthally segmented into 20° modular wedges, and form towers of size 0.175×0.175 in $(\Delta\eta \times \Delta\phi)$. The silicon tracker, consisting of 1856 silicon pixel and 15 148 silicon strip detector modules, measures charged particles within $|\eta| < 2.4$. For nonisolated particles with transverse momentum $1 < p_T < 10$ GeV/c and $|\eta| < 1.4$, the typical track momentum resolution is 1.5%, and the transverse (longitudinal) impact parameter resolution ranges from 25–90 (45–150) μm. The CMS detector response is simulated in detail using Geant4 [17].

3. Event and track selections

Events from XeXe collisions are selected at the hardware level (level-1) by requiring the presence of both colliding bunches at the nominal interaction point [18]. A minimum energy deposit is required in at least one HF calorimeter tower, optimized to maximize event acceptance while suppressing noise from electromagnetic scattering and pileup (multiple interactions in a single bunch crossing). Pileup is negligible because the average number of collisions per bunch crossing is 0.018. At the high-level trigger [19], at least one reconstructed track in the pixel detector is required. Offline event selection further requires a minimum energy deposit of 3 GeV in each of at least three HF towers on both sides of the detector, to enhance selection of hadronic collisions and suppress ultraperipheral electromagnetic interactions. Events must contain a reconstructed primary vertex with at least two tracks, and located within 15 cm along the beam axis and 0.2 cm transversely relative to the nominal collision region. To reduce beam-gas interaction contamination, events with more than ten tracks must have at least 25% of tracks meeting high-purity quality criteria [15]. The overall event selection efficiency for hadronic events is approximately 95%. Track reconstruction follows algorithms similar to those used in proton-proton collisions [15].

For PbPb collisions, a cluster shape filter in the pixel detector ensures compatibility with particles originating from the primary vertex. The pileup rate is negligible (on average 0.0005 collisions per bunch crossing). Events are selected by requiring energy deposits of at least 4 GeV in two HF towers on both sides of the interaction point, favoring hadronic collisions. The same vertex location criteria as in XeXe data are used. Track reconstruction for the PbPb data utilizes a deep neural network algorithm trained with input variables including normalized χ^2 per degree of freedom, p_T resolution, and number of hits in the silicon pixel and strip detectors, based on conditions of the CMS detector from the reconstruction of earlier 2018 PbPb data [18].

In both the XeXe and PbPb systems, the analysis is restricted to primary charged particle tracks with $|\eta| < 2.4$ and $0.5 < p_T < 3.0$ GeV/c. For XeXe data, tracks are required to have impact parameter significances with respect to the primary vertex less than three standard deviations in both the beam direction (d_z) and the transverse plane (d_0), as well as a relative p_T uncertainty $\sigma_{p_T}/p_T < 10\%$. For PbPb data, the neural-network-based reconstruction imposes requirements on d_z and d_0 similar to those used for XeXe data [15,20].

In this Letter, all observables are presented as functions of centrality, which is related to the degree of geometric overlap of the two colliding nuclei. The centrality percentage represents the fraction of the total inelastic hadronic cross section. A 0% centrality corresponds to a fully head-on collision, while higher centrality percentages indicate more peripheral collisions with smaller overlap. Experimentally, centrality is determined using the percentiles of the energy deposited in the HF calorimeters [21].

4. Analysis techniques

The two-particle correlation and multiparticle cumulant methods are discussed in Ref. [18]. In the two-particle correlation analyses, a charged particle from one p_T interval (the "trigger" particle) is paired with all of the remaining charged particles from the same p_T interval (the "associated" particles).

For a given trigger particle, the pairing is performed in two-dimensional (2D) bins of differences in η and azimuthal angle $(\Delta\eta, \Delta\phi)$. The signal and mixed-event distributions are defined as the per-trigger-particle yield of pairs in the same or mixed events:

$$S(\Delta\eta, \Delta\phi) = \frac{1}{N_{\text{trig}}} \frac{\mathrm{d}^2 N^{\text{same}}}{\mathrm{d}\Delta\eta\, \mathrm{d}\Delta\phi}$$
$$M(\Delta\eta, \Delta\phi) = \frac{1}{N_{\text{trig}}} \frac{\mathrm{d}^2 N^{\text{mixed}}}{\mathrm{d}\Delta\eta\, \mathrm{d}\Delta\phi}, \quad (4)$$

where N^{same} (N^{mixed}) is the number of same- (mixed-) event particle pairs in a given $(\Delta\eta, \Delta\phi)$ bin and N_{trig} is the number of trigger particles.

The mixed-event distribution is used to estimate the random combinatorial background and is constructed by pairing trigger particles in an event with associated particles from ten other randomly chosen events. Events are considered for mixing only if they belong to the same centrality bin (with a bin width of 5% or 10%) and the difference in their primary vertex locations along the beam axis is less than 2 cm.

The per-trigger-particle associated yield used to extract the v_n coefficients is found by normalizing the ratio of the signal and mixed-event distributions:

$$\frac{1}{N_{\text{trig}}} \frac{\mathrm{d}^2 N^{\text{pair}}}{\mathrm{d}\Delta\eta \mathrm{d}\Delta\phi} = M(0,0) \frac{S(\Delta\eta, \Delta\phi)}{M(\Delta\eta, \Delta\phi)}, \quad (5)$$

where $M(0,0)$ is the mixed-event value at $(\Delta\eta, \Delta\phi) = (0,0)$. This 2D normalized yield is then projected onto $\Delta\phi$ before fitting to a Fourier expansion. A selection of $|\Delta\eta| > 2$ is applied to suppress short-range nonflow correlations such as jets [22]. The fitting is done using:

$$\frac{1}{N_{\text{trig}}} \frac{\mathrm{d}N^{\text{pair}}}{\mathrm{d}\Delta\phi} = \frac{N_{\text{assoc}}}{2\pi} \left(1 + \sum_n 2V_{n\Delta} \cos(n\Delta\phi)\right), \quad (6)$$

where N_{assoc} is the number of associated particles in the selected kinematic interval, and $V_{n\Delta}$ denotes the nth Fourier coefficient.

Under the factorization assumption [23], $V_{n\Delta}(\mathrm{p}_T^a, \mathrm{p}_T^b) = v_n(\mathrm{p}_T^a)\, v_n(\mathrm{p}_T^b)$, and for trigger and associated particles from the same p_T range, the nth flow harmonic is extracted as:

$$v_n\{2, |\Delta\eta| > 2\} = \sqrt{V_{n\Delta}}, \tag{7}$$

where the first "2" in the v_n variable list refers to flow harmonics from two-particle correlations.

Multiparticle correlations involving four or more particles are studied with the Q-cumulant method [24], which incorporates track-by-track weights to correct for detector acceptance and efficiency [25]. This method allows the computation of cumulants that probe genuine multiparticle azimuthal correlations. Here, "genuine" correlations refer to irreducible multiparticle correlations that cannot be factorized into products of lower-order correlations, thereby providing sensitivity to collective behavior while suppressing nonflow contributions.

Within this framework, the four-particle v_n, $v_n\{4\}$, are extracted from four-particle cumulants. The two-particle cumulant $c_n\{2\}$ and four-particle cumulant $c_n\{4\}$ are defined as:

$$c_n\{2\} = \langle\langle e^{in(\phi_1-\phi_2)}\rangle\rangle,\ c_n\{4\} = \langle\langle e^{in(\phi_1+\phi_2-\phi_3-\phi_4)}\rangle\rangle - 2\,c_n\{2\}^2, \tag{8}$$

where $\langle\langle\cdots\rangle\rangle$ denotes an average performed in two steps: (i) first over all particles within a single event, and (ii) then over all events [24]. The corresponding four-particle cumulant is then obtained as

$$v_n\{4\} = \sqrt[4]{-c_n\{4\}}. \tag{9}$$

Four-particle symmetric cumulants (SC) measure correlations between the squared flow coefficients of two different harmonics, n and m:

$$\begin{aligned}\mathrm{SC}(n,m) &= \langle\langle\cos(n\phi_1 + m\phi_2 - n\phi_3 - m\phi_4)\rangle\rangle \\ &\quad - \langle\langle\cos[n(\phi_1-\phi_2)]\rangle\rangle\langle\langle\cos[m(\phi_1-\phi_2)]\rangle\rangle \\ &= \langle v_n^2 v_m^2\rangle - \langle v_n^2\rangle\langle v_m^2\rangle.\end{aligned} \tag{10}$$

This technique, originally introduced in Ref. [26], follows the same framework as described in Ref. [25]. The SC observable isolates correlations between fluctuations of flow harmonics beyond trivial statistical fluctuations. Similarly, symmetric cumulants of six particles [$\mathrm{SC}(k,l,m)$] involve combinations of the second orders of three different v_n coefficients [27].

Higher-order mixed harmonic cumulants (MHC) involving six or eight particles, also called m-observable cumulants [28] and first studied in Ref. [22], provide further suppression of nonflow correlations and probe the nonlinear hydrodynamic response and mode-coupling effects between different flow harmonics with enhanced sensitivity [22,28]. For example, the six-particle MHC involving v_2^4 and v_3^2 is defined as:

$$\mathrm{MHC}(v_2^4, v_3^2) = \langle v_2^4 v_3^2\rangle - 4\langle v_2^2 v_3^2\rangle\langle v_2^2\rangle - \langle v_2^4\rangle\langle v_3^2\rangle + 4\langle v_2^2\rangle^2\langle v_3^2\rangle. \tag{11}$$

By construction, an m-particle cumulant removes contributions from correlations involving fewer than m particles, thereby reducing contamination from nonflow sources such as jets or resonance decays even further [28]. Similar cumulants can be defined for combinations of different orders of v_2 and v_3, and also v_2 and v_4, following the prescription in Ref. [22].

To enable more direct comparisons between different collision systems and between data and theoretical calculations, normalized cumulants are used. The normalized four- and six-particle symmetric cumulants (NSC) are defined as:

$$\mathrm{NSC}(n,m) = \frac{\mathrm{SC}(n,m)}{\langle v_n^2\rangle\langle v_m^2\rangle} \tag{12}$$

$$\mathrm{NSC}(k,l,m) = \frac{\mathrm{SC}(k,l,m)}{\langle v_k^2\rangle\langle v_l^2\rangle\langle v_m^2\rangle}. \tag{13}$$

These normalizations improve the comparison between different collision systems and with theoretical predictions. They do so by removing dependencies on the magnitudes of the flow coefficients, which can depend, for example, on the average p_T.

The normalized MHC (nMHC) scale the MHC by the average flow coefficients as:

$$\mathrm{nMHC}(v_m^k, v_n^l) = \frac{\mathrm{MHC}(v_m^k, v_n^l)}{\langle v_m^k\rangle\langle v_n^l\rangle} \tag{14}$$

$$\mathrm{nMHC}(v_m^k, v_n^l, v_p^q) = \frac{\mathrm{MHC}(v_m^k, v_n^l, v_p^q)}{\langle v_m^k\rangle\langle v_n^l\rangle\langle v_p^q\rangle}. \tag{15}$$

All cumulants are calculated using a $|\Delta\eta| > 2$ selection in both the numerator and denominator of the normalized cumulants, further reducing residual nonflow effects. The two–particle correlation method is retained for $v_n\{2, |\Delta\eta| > 2\}$ because it provides improved statistical precision while maintaining the same large pseudorapidity separation. In this regime, short-range correlations are strongly suppressed, and the resulting $v_n\{2, |\Delta\eta| > 2\}$ values are consistent with those obtained from the two–particle cumulant technique within the quoted systematic uncertainties. These small differences do not affect the conclusions found from the model–data comparisons.

The full mathematical details and further discussion of these methods can be found in Refs. [18,22,24].

5. Systematic uncertainties

Systematic uncertainties are evaluated from four main sources for both XeXe and PbPb collisions. Only the maximum relative uncertainties across all observables are quoted below, with the largest values found for measurements involving v_4. In the following, percentage uncertainties are listed for XeXe collisions first, followed by the value for PbPb collisions. First, the track selection criteria are varied by comparing results using tighter (impact parameter significance < 2 standard deviations, relative p_T uncertainty < 5%) and looser (5 standard deviations and 15%) selections, resulting in maximum uncertainties of 6 and 5%. Second, uncertainties from the primary vertex position are estimated by comparing results with vertex positions along the beam axis in the ranges $|z_{\text{vtx}}| < 3$ cm and $3 < |z_{\text{vtx}}| < 15$ cm, yielding uncertainties up to 6 and 5% in the centrality range 0–10%. Third, centrality calibration uncertainties, assessed by varying event selection criteria [18], contribute up to 6 and 3% in peripheral events. Finally, discrepancies between original track distributions generated by the HYDJET model [29] and those obtained after full detector simulation, reconstruction, and efficiency corrections produce systematic uncertainties up to 9 and 5%. The centrality dependence of these uncertainties varies with the analysis method: in two-particle correlations, the largest uncertainties appear in central collisions (9% for $v_4\{2, |\Delta\eta| > 2\}$), while in multiparticle cumulants, the maximum relative uncertainty is about 6% in mid-central to peripheral collisions. Overall, the various v_n coefficients show consistent systematic trends, with partial cancellation in the cumulant results due to correlations between numerator and denominator terms defined in Eqs. (12) to (15).

6. Description of the models

The IP-GLASMA initial-condition (IC) model is an event generator incorporating event-by-event geometric and subnucleonic quantum fluctuations through dependencies on the impact parameter and the longitudinal momentum fraction x, where x denotes the fraction of a nucleon's momentum carried by a quark or gluon in a high energy scattering process [30]. This model captures the fluctuating color charge configurations in ultrarelativistic nuclear collisions. The model has been shown to accurately reproduce experimental features of odd flow harmonics, particularly v_3, which are known to be dominated by initial-state fluctuations [30].

The full IP-GLASMA + MUSIC + URQMD framework [31] builds upon the fluctuating initial states from IP-GLASMA-IC by incorporating hydrodynamic evolution using MUSIC [32], a second-order relativistic viscous

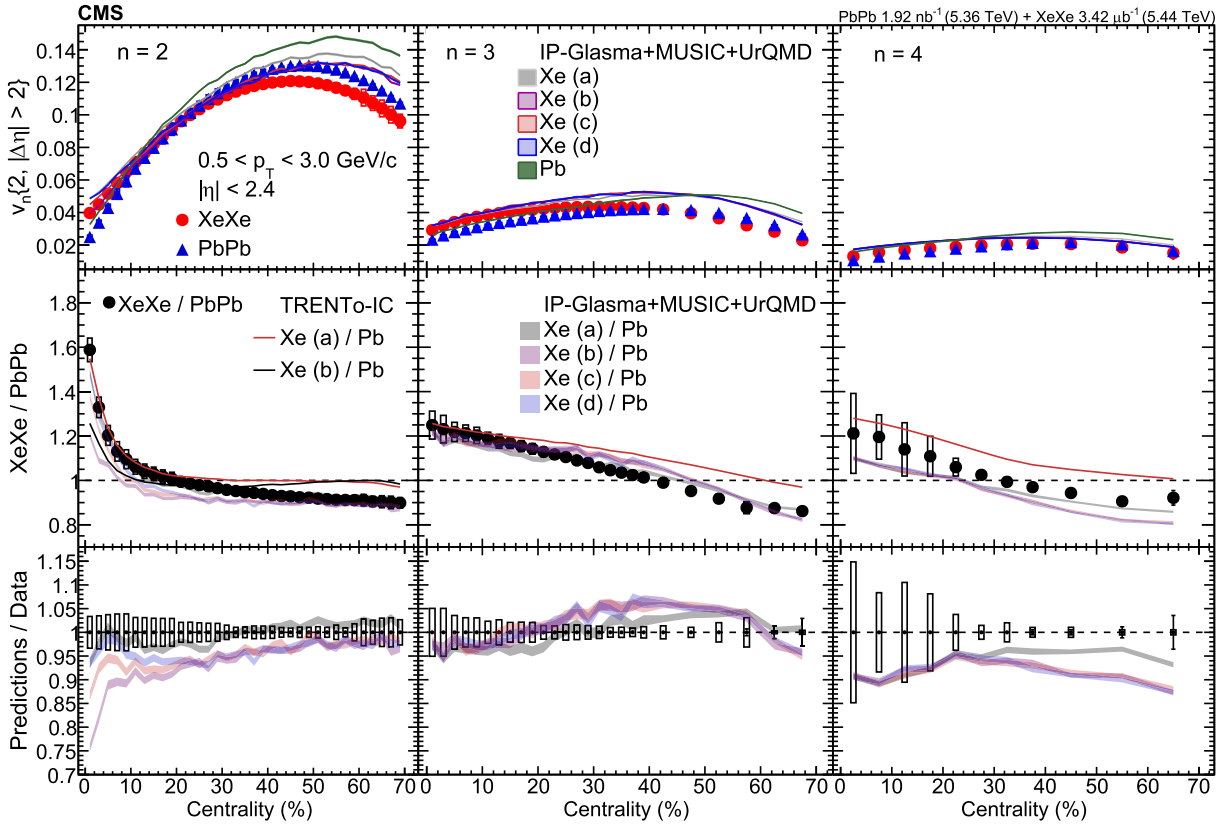

Fig. 1. The upper row shows $v_n\{2, |\Delta\eta| > 2\}$ for elliptic ($n = 2$, left), triangular ($n = 3$, middle), and quadrangular ($n = 4$, right) flow, as a function of centrality in XeXe and PbPb collisions, calculated using the 2-particle correlation method. The vertical bars (mostly smaller than the marker size) and the open boxes represent the statistical and systematic uncertainties, respectively. The shaded bands represent five different hydrodynamic predictions from the IP-GLASMA + MUSIC + URQMD model using four Xe parameter sets, and one Pb parameter set; the band widths indicate the statistical uncertainties of the model calculations. Some model predictions in the upper row are partially obscured due to overlap with others. The middle row compares various theoretical predictions to the data for the XeXe/PbPb ratios. The red and black solid lines show predictions using ratios of the initial-state eccentricities ε_n from the TRENTO-IC model with deformed (Xe (a)) and spherical (Xe (b)) parameters, respectively, both taken as ratios with respect to the Pb nucleus. The lower row shows the ratios of the hydrodynamic predictions to data.

Table 1
Woods–Saxon parameters used to model the nuclear density distributions for the ^{129}Xe nucleus in four different deformation configurations and for the ^{208}Pb nucleus. The parameters R_0, a_0, β_2, and β_4 are defined in Eq. (3).

Nucleus	R_0 (fm)	a_0 (fm)	β_2	β_4
Xe (a)	5.601	0.492	0.207	- 0.003
Xe (b)	5.420	0.570	0.000	- 0.003
Xe (c)	5.420	0.570	0.162	- 0.003
Xe (d)	5.420	0.570	0.207	- 0.003
Pb	6.647	0.537	0.006	0.000

hydrodynamic program. The MUSIC simulation employs a fixed specific shear viscosity to entropy density ratio $\eta/s = 0.12$ and a temperature-dependent bulk viscosity $\zeta/s(T)$ for the QGP phase until hadronization. Afterward, resonance decays and hadronic rescattering are simulated with URQMD v3.4 [33,34] until kinetic freeze-out.

For this analysis, four sets of Woods–Saxon deformation parameters for Xe and one set for Pb are used. These deformation parameters originate from both theoretical calculations and empirical studies, and were provided by the authors of Ref. [30]. They are intended to span a representative range of plausible nuclear deformations for the Xe nuclei and are summarized in Table 1.

The TRENTO-IC model [35] is an initial-state model that does not assume any specific mechanism for pre-equilibrium dynamics, or thermalization. It deposits entropy in proportion to the generalized (typically geometric) mean of the nuclear overlap density between the colliding nuclei. This model simulates only the initial-state eccentricities, ε_n, and does not consider any final-state effects like hydrodynamic evolution or hadronic scattering. Eccentricities for XeXe collisions are found using only two sets of deformation parameters, Xe (a) for deformed and Xe (b) for spherical configurations.

7. Results

7.1. Sensitivity to nuclear deformation of the Xe nucleus

Fig. 1 presents the 2-particle correlation results for $v_n\{2, |\Delta\eta| > 2\}$ with $n = 2, 3, 4$ as a function of centrality for XeXe and PbPb collisions. The upper, middle, and lower rows show the v_n values, comparisons of model predictions to the data, and the ratios of the hydrodynamic model predictions to the data, respectively.

All three flow harmonics exhibit larger values in XeXe events than in PbPb data for lower centrality percentages, which correspond to more central collisions, but smaller values in peripheral collisions. This enhancement of v_2 in central XeXe collisions is likely driven by the quadrupole deformation of the Xe nucleus, while the larger v_3 compared to PbPb indicates stronger initial-state density fluctuations in XeXe [36]. In central collisions, enhanced values of v_4 in XeXe relative to PbPb col-

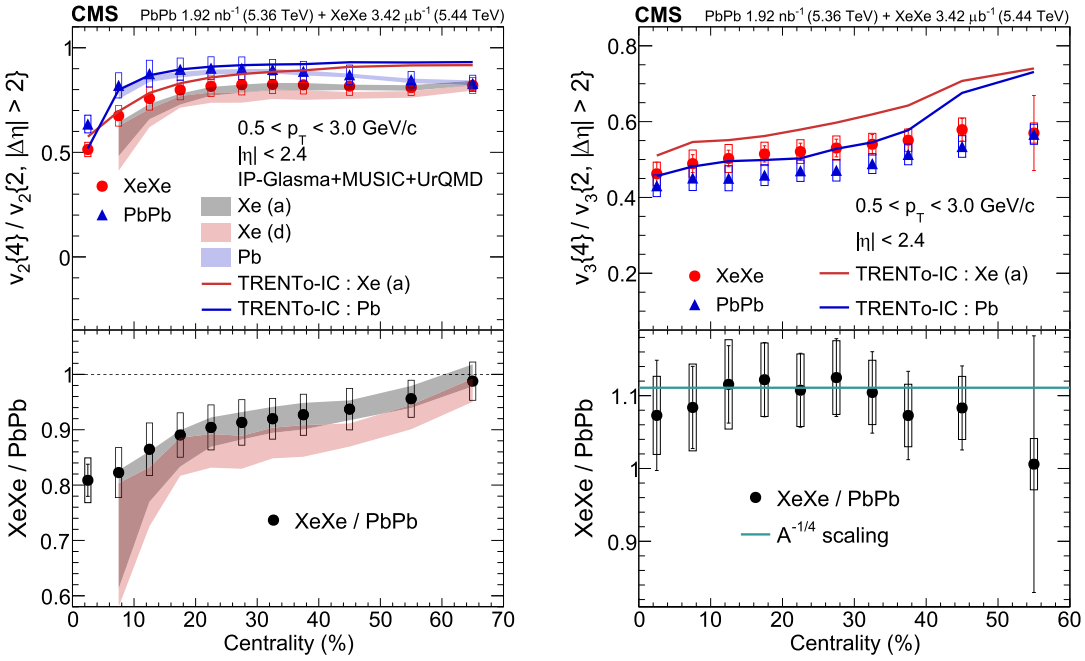

Fig. 2. The upper panels show $v_n\{4\}/v_n\{2, |\Delta\eta| > 2\}$ for elliptic ($n = 2$, left) and triangular ($n = 3$, right) flow, calculated from multiparticle cumulants, as a function of centrality in XeXe and PbPb collisions. The vertical bars (mostly smaller than the marker size) on the dots and the open boxes represent the statistical and systematic uncertainties in the data, respectively. The red and blue solid lines show the predictions from TRENTo-IC in terms of the initial-state eccentricities ε_n for deformed Xe (a) and Pb nuclei. The shaded bands show the hydrodynamic predictions from the IP-Glasma + music + UrQMD model for Xe (a) and Xe (d); the band widths indicate the statistical uncertainties of the model calculations. The lower panels display the ratio of the XeXe to the PbPb results. The cyan line in the lower right panel shows the theoretical prediction for $v_3\{4\}/v_3\{2, |\Delta\eta| > 2\}$ based on $A^{-1/4}$ scaling.

lisions can be interpreted as arising from larger event-by-event fluctuations. In contrast, in mid-central and peripheral collisions, v_4 is dominated by nonlinear coupling to v_2 [36,37]. Since v_2 is smaller in XeXe than in PbPb in this centrality range, the resulting nonlinear contribution to v_4 is reduced in XeXe, leading to XeXe/PbPb v_4 ratios below unity [36].

The middle row of Fig. 1 compares the XeXe/PbPb ratios to IP-Glasma + music + UrQMD and TRENTo-IC model predictions. The IP-Glasma + music + UrQMD hydrodynamic predictions are given for four Xe nuclear shape parameter sets [30], with statistical uncertainties shown as shaded bands. The TRENTo-IC model predicts the initial-state eccentricities ε_n and their ratios. The comparison to v_n ratios assumes an approximately linear hydrodynamic response, $v_n \propto \varepsilon_n$, such that the flow ratios qualitatively reflect the corresponding eccentricity ratios. The predictions are displayed in Fig. 1 for v_2 using the Xe (a) and (b) sets, but only with the Xe (a) set for v_3 and v_4 due to their insensitivity to elliptical deformation. For a clearer comparison, the lower row in Fig. 1 displays the ratios of the hydrodynamic model predictions to data. Ratios are not shown for the TRENTo-IC model, as it provides initial-state eccentricities, while the ratios presented here involve final-state flow observables.

For the hydrodynamic model with parameter set (a), the largest value of the quadrupole deformation β_2 gives the best agreement for v_2 with a reduced $\chi^2/NDF \approx 0.99$, compared to values from 4.6 to 8.5 for the other sets. Set (d), having the same β_2 as set (a) but a larger value for the nuclear skin depth a_0, describes the data slightly better than sets (b) or (c) for the 0—10% most central events ($\chi^2/NDF \approx 4.6$, as opposed to values of about 8.5 and 5.0 for sets (b) and (c), respectively). For v_3, set (a) also fits best ($\chi^2/NDF \approx 1.7$, compared to $\chi^2/NDF > 4$ for the others) for the 20–70% centrality region, but is comparable or even slightly worse in other centrality regions. In the case of v_4, all 4 sets give comparable predictions for the 0–20% centrality region, but set (a) performs best in the 20–70% centrality region ($\chi^2/NDF \approx 6.8$ overall, compared to $\chi^2/NDF > 20$ for the others).

The TRENTo-IC model gives a poor description of v_2 for peripheral events (beyond about 35–40% centrality) and fails to match v_3 and v_4 overall (except for extremely central collisions). These discrepancies are likely due to viscous damping effects, which are stronger in the smaller XeXe system [36]. However, for v_2 in the 0–20% centrality region, which is more sensitive to deformation, the predictions using the deformed Xe (a) parameters show better agreement with the data. In fact, this agreement is comparable to that for the hydrodynamic model using the same Xe parameter set.

Differences between models and data may arise from multiple factors. Integrated flow harmonics can be over- or underestimated due to differences in the p_T ranges, affecting extraction of QGP transport coefficients [η/s, $\zeta/s(T)$] [38]. The IP-Glasma + music + UrQMD simulations use $\eta/s = 0.12$, but theoretical uncertainties remain. The models also assume values of zero for both the octupole deformation (β_3) and triaxiality (γ) parameters, the latter describing deviations from axial symmetry. However, recent studies suggest that Xe nuclei exhibit large deformation fluctuations due to a second-order phase transition along the Xe isotope chain [39], which these models do not account for. Uncertainties in freeze-out criteria further impact predicted flow observables, contributing to discrepancies and uncertainties in extracting the Xe deformation parameters. In addition, in peripheral collisions, contributions from non-thermalized or pp-like (core—corona) events may influence the measured correlations, effects which are not fully captured by the hydrodynamic models [40]. While such contributions may partially cancel in the XeXe/PbPb ratios, some residual effects may remain due to differences in system size and geometry [41].

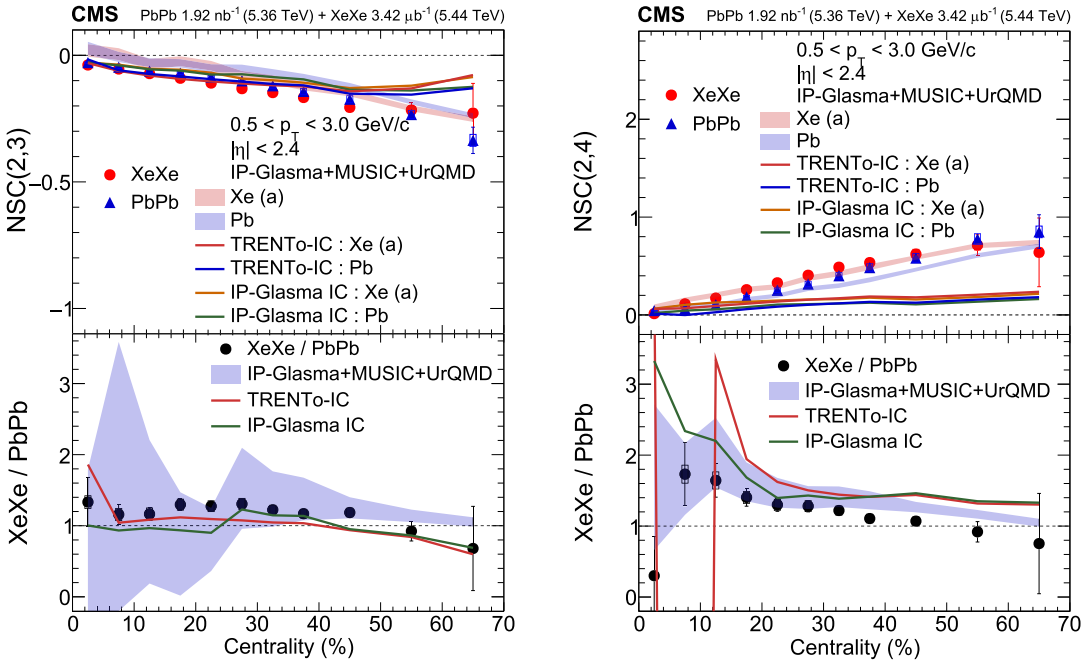

Fig. 3. The upper panels show the normalized symmetric cumulants NSC(2, 3) (left) and NSC(2, 4) (right) as functions of centrality in XeXe and PbPb collisions, calculated from multiparticle cumulants. The vertical bars and the open boxes represent the statistical and systematic uncertainties, respectively. The red and blue solid lines show the predictions from TRENTo-IC in terms of initial-state eccentricities ε_n for deformed Xe (Xe (a)) and Pb nuclei. The orange and green solid lines show the predictions from the IP-Glasma-IC model with the same Xe and Pb nucleus parameters. The shaded bands show the hydrodynamic predictions from the IP-Glasma + music + UrQMD model; the band widths indicate the statistical uncertainties of the model calculations. The lower panels display the corresponding ratios of NSC(m, n) for XeXe/PbPb. The red solid lines show the initial-state predictions from TRENTo-IC, while the green solid lines show those from IP-Glasma-IC. The blue shaded band is the hydrodynamic prediction from IP-Glasma + music + UrQMD. In the 5–10% centrality range, the TRENTo-IC NSC(2, 4) ratio is negative because the PbPb prediction lies just below zero.

The observable $v_n\{4\}/v_n\{2, |\Delta\eta| > 2\}$ provides direct information about event-by-event fluctuations of v_n [36]. If v_n fluctuates between events, this ratio is smaller than 1. The values of $v_2\{4\}/v_2\{2, |\Delta\eta| > 2\}$ exhibit a significant centrality dependence, as shown in the upper left panel of Fig. 2, with the largest deviation from unity occurring in more central events. The systematically larger deviations from unity in XeXe compared to PbPb events indicate larger elliptic flow fluctuations in XeXe collisions. These trends are also observed in both the initial-state TRENTo-IC and hydrodynamic IP-Glasma + music + UrQMD predictions. In Ref. [38], this observable was shown to be sensitive to a_0, which characterizes the degree of nuclear diffuseness. A smaller a_0 corresponds to a sharper nuclear surface, which reduces event-by-event fluctuations of the initial elliptic geometry, particularly in semi-central collisions. As a result, the $v_2\{4\}/v_2\{2, |\Delta\eta| > 2\}$ ratio is less suppressed [38].

To further investigate this sensitivity, the double ratio of $v_2\{4\}/v_2\{2, |\Delta\eta| > 2\}$ for XeXe to PbPb values is shown in the lower left panel of Fig. 2. The theoretical predictions using parameter set Xe (a) with $a_0 = 0.492$ more closely match the data than set (d) with $a_0 = 0.570$, reinforcing the conclusion based on $v_2\{2, |\Delta\eta| > 2\}$ alone.

In the following discussion, the IP-Glasma + music + UrQMD predictions for XeXe collisions will use only parameter set Xe (a), which provides the closest match to data. For higher-order cumulants, all parameter sets remain compatible within the uncertainties.

7.2. Nonlinear hydrodynamic response through higher-order moments of flow harmonics

The upper left panel in Fig. 2 also shows that the ratios $\varepsilon_2\{4\}/\varepsilon_2\{2\}$ from TRENTo-IC (solid lines) exceed the corresponding v_2 ratios in more peripheral collisions, indicating a nonlinear hydrodynamic response that increases towards peripheral collisions [7]. This effect is more pronounced in XeXe collisions (starting from around 30% centrality, as opposed to 50% centrality in PbPb collisions), suggesting stronger nonlinearity in the smaller XeXe system. The same nonlinear response is also observed in the upper right panel of Fig. 2, where the predictions from TRENTo-IC for $\varepsilon_3\{4\}/\varepsilon_3\{2\}$ (solid lines) exceed the corresponding v_3 ratios. In contrast to what was seen for v_2, the values of $v_3\{4\}/v_3\{2, |\Delta\eta| > 2\}$ for both the predictions and the data are closer to unity for XeXe than for PbPb collisions. Finite-size corrections to the central limit theorem, which induce non-Gaussian fluctuations in the initial triangularity ε_3, were predicted to result in an $A^{-1/4}$ scaling of $v_3\{4\}/v_3\{2, |\Delta\eta| > 2\}$ (where A is the atomic mass number) [36]. The non-Gaussian fluctuations scale with the number of participant nucleons, which roughly scales with A, leading to the observed scaling behavior. The lower right panel in Fig. 2 shows the XeXe/PbPb ratio, with the cyan line representing $(129/208)^{-1/4} \approx 1.13$, which agrees with the data within uncertainties.

The actual values of $v_2\{4\}$ and $v_3\{4\}$, without normalization by $v_n\{2, |\Delta\eta| > 2\}$, are given in Appendix A.

7.2.1. Normalized symmetric cumulants involving two or three flow harmonics

Fig. 3 presents the normalized four-particle symmetric cumulants involving two harmonics, NSC(2, 3) (left) and NSC(2, 4) (right), as functions of centrality in XeXe and PbPb collisions. In order to suppress nonflow effects, these are calculated using two particles from each of two separated η regions: $-2.4 < \eta < -1$ and $1 < \eta < 2.4$. The NSC(2, 3) values probe the interplay between elliptic and triangular fluctuations

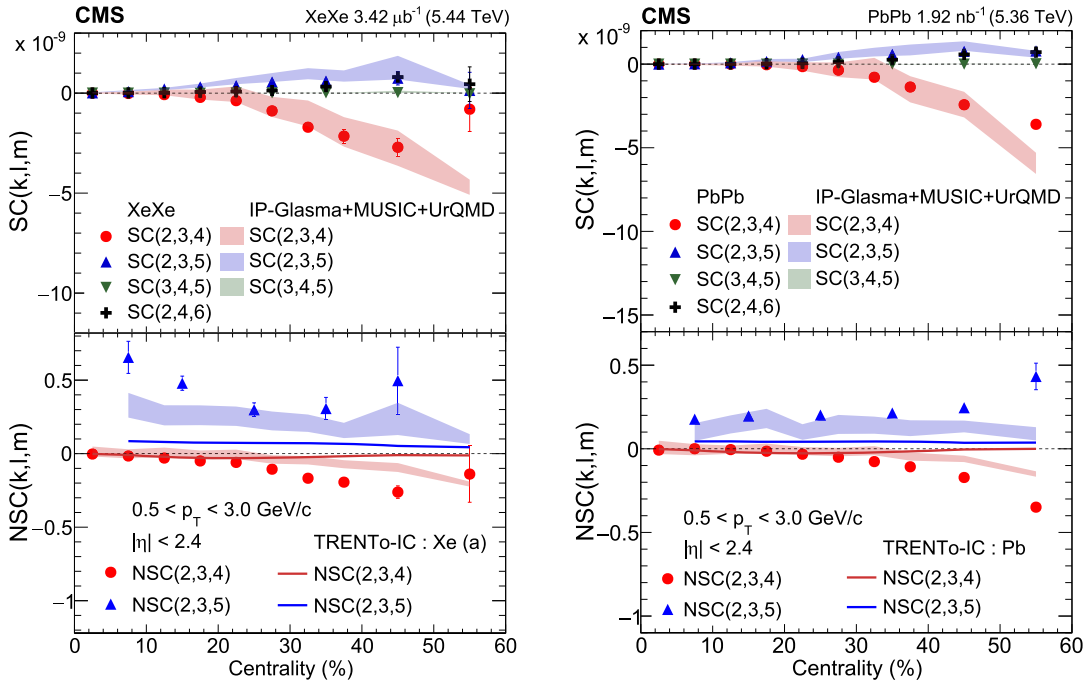

Fig. 4. A selection of six-particle three-harmonic SC and NSC cumulants as functions of centrality in XeXe (left) and PbPb (right) collisions, calculated from multiparticle cumulants. The vertical bars represent the statistical uncertainties, with the systematic uncertainties being negligible. The shaded bands show hydrodynamic predictions from the IP-Glasma + music + UrQMD model for the Xe (a) deformed nuclear shape parameters and for the spherical Pb nucleus; the band widths indicate the statistical uncertainties of the model calculations. The solid lines represent initial-state model predictions from TRENTo-IC.

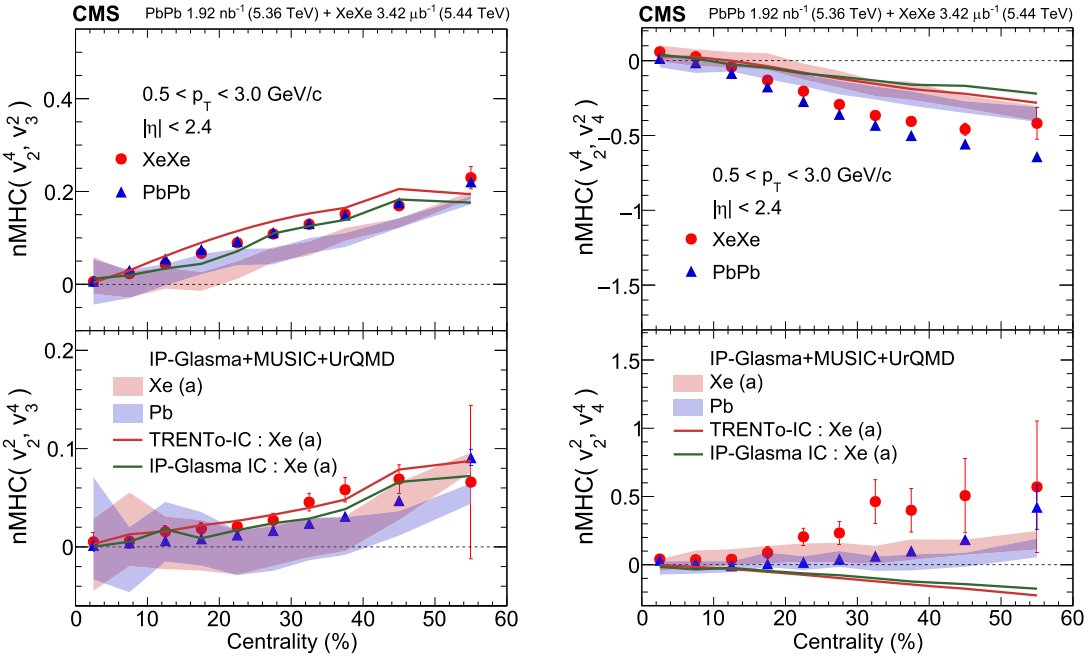

Fig. 5. Six-particle normalized mixed harmonic cumulants (nMHC) as functions of centrality in XeXe and PbPb collisions, calculated from multiparticle cumulants. Upper panels: nMHC(v_2^4, v_3^2) (left) and nMHC(v_2^4, v_4^2) (right). Lower panels: nMHC(v_2^2, v_3^4) (left) and nMHC(v_2^2, v_4^4) (right). The vertical bars represent the statistical uncertainties and the systematic uncertainties are negligible. The shaded bands show hydrodynamic predictions from the IP-Glasma + music + UrQMD model for deformed Xe (Xe (a)) and Pb nuclei; the band widths indicate the statistical uncertainties of the model calculations. The solid lines represent initial-state model predictions.

influenced by eccentricities and deformation, while NSC(2, 4) is sensitive to nonlinear mode couplings and higher-multipole nuclear deformations (e.g., β_4), providing complementary constraints on the initial geometry. The results show that v_2^2 and v_3^2 are anticorrelated across all centralities, reflecting the anticorrelation between initial eccentricities ε_2 and ε_3, whereas v_2^2 and v_4^2 are positively correlated due to nonlinear mode coupling, where v_4 receives contributions proportional to ε_2^2 [22]. The lower panels display the XeXe/PbPb ratios of NSC(2, 3) and NSC(2, 4), highlighting the differences between the initial states of the two systems.

The IP-Glasma + music + UrQMD hydrodynamic model captures the trends of both NSC(2, 3) and NSC(2, 4), albeit with a slight underestimation of the deviation from zero in some cases. Initial-state TRENTo-IC and IP-Glasma-IC models reproduce NSC(2, 3) except in peripheral collisions, where the linear relations $v_2 \propto \varepsilon_2$ and $v_3 \propto \varepsilon_3$ slightly break down [7]. For NSC(2,4), initial-state models increasingly underestimate the data from central to peripheral collisions, highlighting that these models lack the dynamical nonlinear mode-coupling generated during hydrodynamic expansion, through which v_4 receives a significant contribution proportional to ε_2^2.

For the XeXe/PbPb ratios shown in the lower row of Fig. 3, IP-Glasma + music + UrQMD, IP-Glasma-IC, and TRENTo-IC all give roughly comparable agreement with the NSC(2, 3) data, with different models being closer to the data in different regions of centrality. Surprisingly, the ratios are well described even in the centrality regions where the two IC models fail to reproduce the individual XeXe and PbPb results. For the NSC(2, 4) ratios, the IP-Glasma + music + UrQMD model gives a reasonable description of the data, while the two IC models (especially the TRENTo-IC model) do notably worse. As was the case for the NSC(2, 3) ratios, the NSC(2, 4) ratios from the IC models are much closer to the data than the individual XeXe and PbPb values. These comparisons highlight the role of NSC(2, 3) and NSC(2, 4) in constraining the initial-state geometry and its fluctuations, helping discriminate between different models of the initial entropy deposition and different sets of nuclear deformation parameters. This is because NSC(2, 3) is highly sensitive to correlations between the initial-state eccentricities ε_2 and ε_3, while NSC(2, 4), through its dependence on v_4, probes higher-order geometric structure and nonlinear mode-mixing effects.

Fig. 4 presents six-particle symmetric cumulants SC(k, l, m) and their normalized counterparts NSC(k, l, m) versus centrality for XeXe collisions (left) measured for the first time, and PbPb collisions (right). The upper rows display SC(2, 3, 4), SC(2, 3, 5), SC(3, 4, 5), and SC(2, 4, 6), while the lower rows show NSC(2, 3, 4) and NSC(2, 3, 5) in both systems. These measurements reveal genuine correlations among three different flow harmonics. In particular, the nonzero NSC(2, 3, 4) values indicate fluctuations in the elliptical shape of the nuclear overlap region, beyond mere magnitude fluctuations of elliptic deformation [27]. The NSC(2, 3, 4) values in XeXe and PbPb are similar in the most central collisions, while in the mid-central range (15–45%) the XeXe values are systematically larger in magnitude, suggesting moderately stronger shape fluctuations in the initial geometry. The SC(3, 4, 5) values are consistent with zero in both systems, as seen in Refs. [27,42], while the other SC(k, l, m) cumulants have finite values. Notably, SC(2, 3, 5) and NSC(2, 3, 5) show different trends in XeXe collisions, possibly indicating more nonlinear contribution for v_5 from v_2 and v_3 in the smaller system, with an even larger difference for the NSC data [42].

Hydrodynamic IP-Glasma + music + UrQMD calculations provide an overall good description of the individual SC(k, l, m) observables, but tend to underestimate the values of NSC(k, l, m) in certain centrality intervals. In contrast, the initial-state TRENTo-IC predictions systematically underestimate NSC(k, l, m), with the discrepancy becoming more pronounced toward peripheral collisions. As for the four-particle sym-

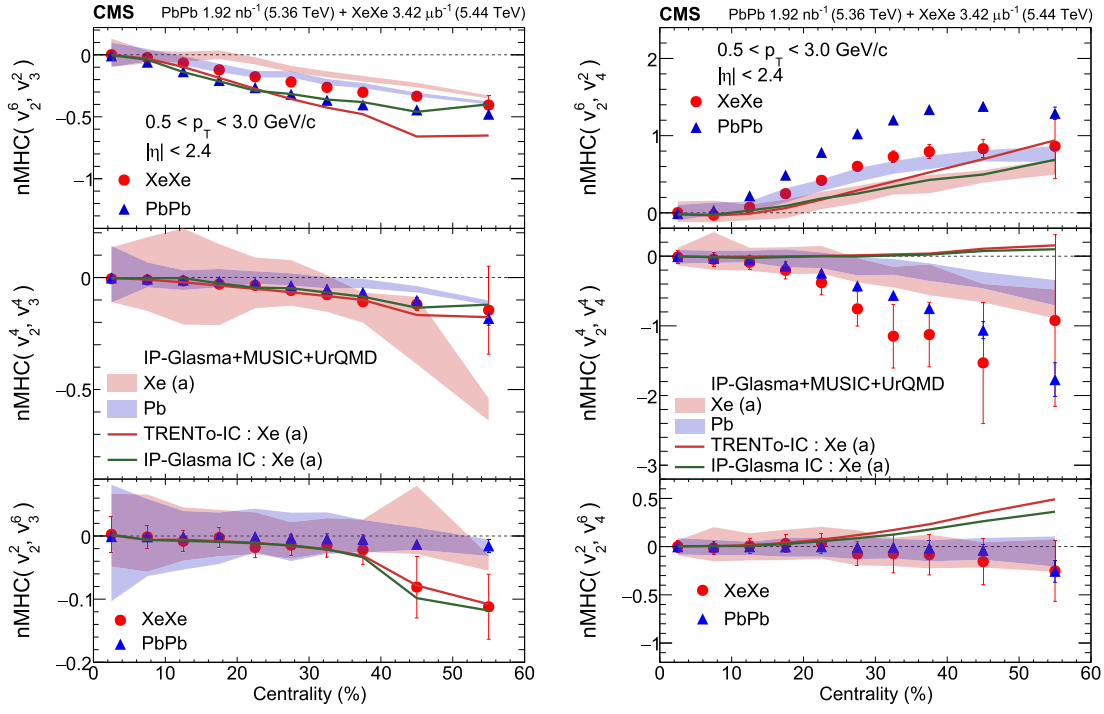

Fig. 6. Eight-particle normalized mixed harmonic cumulants (nMHC) as functions of centrality in XeXe and PbPb collisions, calculated from multiparticle cumulants. Left panels: nMHC(v_2^6, v_3^2) (upper), nMHC(v_2^4, v_3^4) (middle), and nMHC(v_2^2, v_3^6) (lower). Right panels: nMHC(v_2^6, v_4^2) (upper), nMHC(v_2^4, v_4^4) (middle), and nMHC(v_2^2, v_4^6) (lower). The vertical bars represent statistical uncertainties and the systematic uncertainties are negligible. The shaded bands show hydrodynamic predictions from the IP-Glasma + music + UrQMD model for deformed Xe (Xe (a)) and Pb nuclei; the band widths indicate the statistical uncertainties of the model calculations. The solid lines represent initial-state model predictions.

metric cumulants, this behaviour observed in TRENTo-IC predictions is again attributed to the dynamical development of multiharmonic correlations during the hydrodynamic evolution of the medium, in particular due to nonlinear hydrodynamic contributions to v_4 and v_5 arising from v_2 and v_3 [22,42].

7.2.2. Correlations between higher-order moments of two flow harmonics

Figs. 5 and 6 present the first comparisons of nMHC(v_2^k, v_3^l) and nMHC(v_2^k, v_4^l) from XeXe and PbPb collisions for $k, l = 2, 4, 6$. The specific combinations are indicated in each panel. A key observation is that the magnitudes of nMHC(v_2^k, v_4^l) are larger than the corresponding values of nMHC(v_2^k, v_3^l) for the same k and l in both collision systems (note the differences in vertical scale between the left and right panels in both figures). This indicates a stronger correlation between higher order moments of v_2 and v_4, consistent with the trend observed for NSC(2, 4) versus NSC(2, 3). This can be attributed to the fact that both v_2 and v_4 are strongly influenced by the initial-state geometry.

A distinct pattern is observed in the magnitudes of correlations involving v_3:

$$|\text{nMHC}(v_2^6, v_3^2)| > |\text{nMHC}(v_2^4, v_3^2)| > |\text{nMHC}(v_2^4, v_3^4)| > |\text{nMHC}(v_2^2, v_3^4)| > |\text{nMHC}(v_2^2, v_3^6)|, \quad (16)$$

similar to the findings in Ref. [22].

For v_4, the sequence differs slightly, with the second and third terms swapped:

$$|\text{nMHC}(v_2^6, v_4^2)| > |\text{nMHC}(v_2^4, v_4^4)| > |\text{nMHC}(v_2^4, v_4^2)| > |\text{nMHC}(v_2^2, v_4^4)| > |\text{nMHC}(v_2^2, v_4^6)|. \quad (17)$$

Since v_2 and v_4 are strongly correlated, the inequality $|\text{nMHC}(v_2^4, v_4^4)| > |\text{nMHC}(v_2^4, v_4^2)|$ suggests that mode couplings involving equal orders of v_2 and v_4 exhibit stronger correlations.

System-size effects show a consistent trend across different nMHC(v_2^k, v_3^l) and nMHC(v_2^k, v_4^l) combinations. Given that initial-state fluctuations are expected to be stronger in the smaller XeXe system, correlations involving higher-order moments of v_3 and v_4 (v_3^4, v_3^6, v_4^4, v_4^6) correlated with lower-order moments of v_2 (v_2^2) show enhanced values in XeXe data, reflecting their greater sensitivity to fluctuations.

For correlations between v_2 and v_3, the four-, six-, and eight-particle cumulants are found to have negative, positive, and negative correlations, respectively, in both XeXe and PbPb collisions, in qualitative agreement with initial-state TRENTo-IC predictions [43]. For example, comparing the upper left panels of Figs. 3, 5, and 6: NSC(2, 3) (4-particle), nMHC(v_2^4, v_3^2) (6-particle), and nMHC(v_2^6, v_3^2) (8-particle) follow this negative, positive, negative pattern.

However, this pattern does not hold for correlations between v_2 and v_4: correlations involving higher-order moments of v_4 ($l = 4, 6$) swap signs for the same order n-particle cumulant. For instance, nMHC(v_2^4, v_4^2) and nMHC(v_2^2, v_4^4) have negative and positive correlations, respectively, despite both being 6-particle cumulants.

The right hand panels in Figs. 5 and 6 compare the hydrodynamic and initial-state model predictions for correlations of various orders of v_2 and v_4, similar to previous studies using v_2 and v_3 [22]. While the hydrodynamic models qualitatively reproduce all of the observed trends, initial-state models exhibit striking disagreements in the correlations of nMHC(v_2^2, v_4^4), nMHC(v_2^4, v_4^4), and nMHC(v_2^2, v_4^6), predicting correlations opposite in sign to what is observed. This discrepancy likely arises because these observables depend on fourth- and sixth-order moments of v_4, which experience nonlinear hydrodynamic responses to ε_2 that grow towards peripheral collisions. This reinforces the conclusion that correlations between v_2 and v_4 predominantly develop dynamically during system evolution, rather than being fully determined by initial-state correlations. These correlations primarily arise from nonlinear hydrodynamic response and are influenced by transport properties such as shear and bulk viscosities [22].

Table 2 summarizes the signs of the correlations observed for different moments of v_2 and v_3/v_4 as functions of centrality.

Table 2
Signs of correlations between different moments of v_2 and v_3/v_4 as functions of centrality.

n-particle cumulant	Quantity	Correlation sign	Quantity	Correlation sign
4	NSC(2, 3)	-	NSC(2, 4)	+
6	nMHC(v_2^4, v_3^2)	+	nMHC(v_2^4, v_4^2)	-
6	nMHC(v_2^2, v_3^4)	+	nMHC(v_2^2, v_4^4)	+
8	nMHC(v_2^6, v_3^2)	-	nMHC(v_2^6, v_4^2)	+
8	nMHC(v_2^4, v_3^4)	-	nMHC(v_2^4, v_4^4)	-
8	nMHC(v_2^2, v_3^6)	-	nMHC(v_2^2, v_4^6)	- (within uncertainties)

8. Summary

For the first time, individual flow harmonics, two- and three-harmonic correlations, and higher-order mixed harmonic cumulants are measured and compared in detail for xenon-xenon (XeXe) and lead-lead (PbPb) collisions at $\sqrt{s_{NN}} = 5.44$ and 5.36 TeV, respectively. Theoretical predictions of the IP-Glasma + music + UrQMD hydrodynamic model, and the TRENTo-IC and IP-Glasma-IC initial-state models, calculated with various sets of deformation parameters for the ^{129}Xe nucleus, are compared to the data. The final-state model calculation from IP-Glasma + music + UrQMD with nuclear deformation parameters $a_0 = 0.492$ and $\beta_2 = 0.207$ for ^{129}Xe provides the best agreement among tested parameter sets. Here, a_0 is the nuclear skin depth, and β_2 is the quadrupole deformation parameter. This comparison indicates that including a prolate deformation in the parameterization of the ^{129}Xe nuclear shape (in contrast to the doubly magic, nearly spherical ^{208}Pb nucleus) is necessary to reproduce the measured flow observables within the IP-Glasma + music + UrQMD framework.

On the other hand, the difference in initial-state predictions from the TRENTo-IC and IP-Glasma-IC models not only point to the sensitivity of these observables to the pre-equilibrium dynamics needed to model the experimental data, but also to the increasing nonlinearity of the higher-order moments of the flow harmonics in peripheral collisions. While differences between the two initial-state models are visible, a definitive conclusion about their relative performance cannot be drawn, as such a comparison without the inclusion of hydrodynamic evolution and freeze-out stages remains incomplete.

The comparison of higher-order moments in XeXe and PbPb collisions provides insight into the impact of system size and shape on these observables. Measurements involving higher-order moments of fluctuation-driven flow harmonics, such as v_3 and v_4, are, as expected, larger in the smaller XeXe system.

Subtle differences exist between data and model calculations with the current sets of parameters. These differences highlight the importance of fine-tuning the model parameters, including not only the nuclear deformation parameters but also those related to hydrodynamic calculations, such as transport coefficients and freeze-out criteria. Such analyses can significantly improve the overall understanding of initial conditions in heavy ion collisions and transport properties of the quark-gluon plasma created at the LHC. Furthermore, this work provides a data-driven, multi-faceted probe of flow fluctuations, offering direct sensitivity to correlations arising from nonlinear hydrodynamic response.

Data availability

Release and preservation of data used by the CMS Collaboration as the basis for publications is guided by the CMS data preservation, re-use and open access policy.

Declaration of competing interest

The authors declare that they have no known competing financial interests or personal relationships that could have appeared to influence the work reported in this paper.

Acknowledgment

We congratulate our colleagues in the CERN accelerator departments for the excellent performance of the LHC and thank the technical and administrative staffs at CERN and at other CMS institutes for their contributions to the success of the CMS effort. In addition, we gratefully acknowledge the computing centers and personnel of the Worldwide LHC Computing Grid and other centers for delivering so effectively the computing infrastructure essential to our analyses. Finally, we acknowledge the enduring support for the construction and operation of the LHC, the CMS detector, and the supporting computing infrastructure provided by the following funding agencies: SC (Armenia), BMBWF and FWF (Austria); FNRS and FWO (Belgium); CNPq, CAPES, FAPERJ, FAPERGS, and FAPESP (Brazil); MES and BNSF (Bulgaria); CERN; CAS, MoST, and NSFC (China); MINCIENCIAS (Colombia); MSES and CSF (Croatia); RIF (Cyprus); SENESCYT (Ecuador); ERC PRG, TARISTU24-TK10 and MoER TK202 (Estonia); Academy of Finland, MEC, and HIP (Finland); CEA and CNRS/IN2P3 (France); SRNSF (Georgia); BMFTR, DFG, and HGF (Germany); GSRI (Greece); NKFIH (Hungary); DAE and DST (India); IPM (Iran); SFI (Ireland); INFN (Italy); MSIT and NRF (Republic of Korea); MES (Latvia); LMTLT (Lithuania); MOE and UM (Malaysia); BUAP, CINVESTAV, CONACYT, LNS, SEP, and UASLP-FAI (Mexico); MOS (Montenegro); MBIE (New Zealand); PAEC (Pakistan); MES, NSC, and NAWA (Poland); FCT (Portugal); MESTD (Serbia); MICIU/AEI and PCTI (Spain); MOSTR (Sri Lanka); Swiss Funding Agencies (Switzerland); MST (Taipei); MHESI (Thailand); TUBITAK and TENMAK (Türkiye); NASU (Ukraine); STFC (United Kingdom); DOE and NSF (USA).

Individuals have received support from the Marie-Curie program and the European Research Council and Horizon 2020 Grant, contract Nos. 675440, 724704, 752730, 758316, 765710, 824093, 101115353, 101002207, 101001205, and COST Action CA16108 (European Union); the Leventis Foundation; the Alfred P. Sloan Foundation; the Alexander von Humboldt Foundation; the Science Committee, project no. 22rl-037 (Armenia); the Fonds pour la Formation à la Recherche dans l'Industrie et dans l'Agriculture (FRIA) and Fonds voor Wetenschappelijk Onderzoek contract No. 1228724N (Belgium); the Beijing Municipal Science & Technology Commission, No. Z191100007219010, the Fundamental Research Funds for the Central Universities, the Ministry of Science and Technology of China under Grant No. 2023YFA1605804, the Natural Science Foundation of China under Grant No. 12061141002, 12535004, and USTC Research Funds of the Double First-Class Initiative No. YD2030002017 (China); the Ministry of Education, Youth and Sports (MEYS) of the Czech Republic; the Shota Rustaveli National Science Foundation, grant FR-22-985 (Georgia); the Deutsche Forschungsgemeinschaft (DFG), among others, under Germany's Excellence Strategy – EXC 2121 "Quantum Universe" – 390833306, and under project number 400140256 - GRK2497; the Hellenic Foundation for Research and Innovation (HFRI), Project Number 2288 (Greece); the Hungarian Academy of Sciences, the New National Excellence Program - ÚNKP, the NKFIH research grants K 131991, K 133046, K 138136, K 143460, K 143477, K 146913, K 146914, K 147048, 2020-2.2.1-ED-2021-00181, TKP2021-NKTA-64, and 2021-4.1.2-NEMZ_KI-2024-00036 (Hungary); the Council of Science and Industrial Research, India; ICSC – National Research Center for High Performance Computing, Big Data and Quantum Computing, FAIR – Future Artificial Intelligence Research, and CUP I53D23001070006 (Mission 4 Component 1), funded by the NextGenerationEU program (Italy); the Latvian Council of Science; the Ministry of Education and Science, project no. 2022/WK/14, and the National Science Center, contracts Opus 2021/41/B/ST2/01369, 2021/43/B/ST2/01552, 2023/49/B/ST2/03273, and the NAWA contract BPN/PPO/2021/1/00011 (Poland); the Fundação para a Ciência e a Tecnologia, grant CEECIND/01334/2018 (Portugal); the National Priorities Research Program by Qatar National Research Fund; MICIU/AEI/10.13039/501100011033, ERDF/EU, "European Union NextGenerationEU/PRTR", and Programa Severo Ochoa del Principado de Asturias (Spain); the Chulalongkorn Academic into Its 2nd Century Project Advancement Project, the National Science, Research and Innovation Fund program IND_FF_68_369_2300_097, and the Program Management Unit for Human Resources & Institutional Development, Research and Innovation, grant B39G680009 (Thailand); the Kavli Foundation; the Nvidia Corporation; the SuperMicro Corporation; the Welch Foundation, contract C-1845; and the Weston Havens Foundation (USA).

Appendix A. $v_2\{4\}$ and $v_3\{4\}$ vs. centrality

Fig. A.7 shows similar measurements to those given in the upper panels of Fig. 1, but now for $v_2\{4\}$ and $v_3\{4\}$.

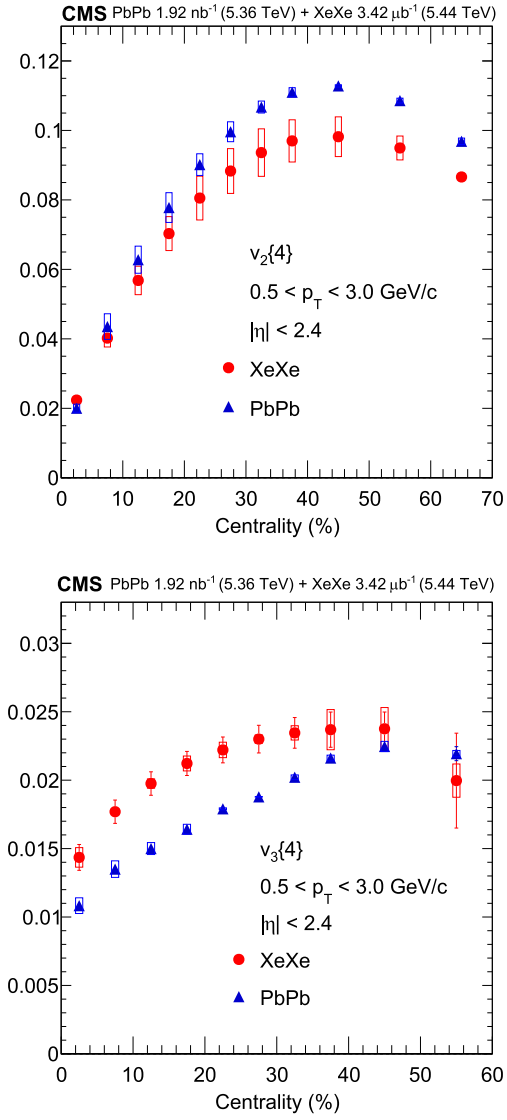

Fig. A.7. Measured $v_2\{4\}$ (upper) and $v_3\{4\}$ (lower) cumulant values as a function of centrality for XeXe and PbPb collisions, calculated using 4-particle cumulants. The vertical bars and open boxes represent the statistical and systematic uncertainties, respectively.

The CMS Collaboration

A. Hayrapetyan[1], V. Makarenko[1], A. Tumasyan[219,1], W. Adam[2], J.W. Andrejkovic[2], L. Benato[2], T. Bergauer[2], M. Dragicevic[2], C. Giordano[2], P.S. Hussain[2], M. Jeitler[220,2], N. Krammer[2], A. Li[2], D. Liko[2], I. Mikulec[2], J. Schieck[220,2], R. Schöfbeck[220,2],

D. Schwarz[2], M. Shooshtari[2], M. Sonawane[2], W. Waltenberger[2], C.-E. Wulz[220,2], T. Janssen[3], H. Kwon[3], D. Ocampo Henao[3], T. Van Laer[3], P. Van Mechelen[3], J. Bierkens[4], N. Breugelmans[4], J. D'Hondt[4], S. Dansana[4], A. De Moor[4], M. Delcourt[4], F. Heyen[4], Y. Hong[4], P. Kashko[4], S. Lowette[4], I. Makarenko[4], D. Müller[4], J. Song[4], S. Tavernier[4], M. Tytgat[221,4], G.P. Van Onsem[4], S. Van Putte[4], D. Vannerom[4], B. Bilin[5], B. Clerbaux[5], A.K. Das[5], I. De Bruyn[5], G. De Lentdecker[5], H. Evard[5], L. Favart[5], P. Gianneios[5], F.A. Khalilzadeh[5], A. Khan[5], A. Malara[5], M.A. Shahzad[5], L. Thomas[5], M. Vanden Bemden[5], C. Vander Velde[5], P. Vanlaer[5], F. Zhang[5], M. De Coen[6], D. Dobur[6], G. Gokbulut[6], J. Knolle[6], L. Lambrecht[6], D. Marckx[6], K. Skovpen[6], N. Van Den Bossche[6], J. van der Linden[6], J. Vandenbroeck[6], L. Wezenbeek[6], S. Bein[7], A. Benecke[7], A. Bethani[7], G. Bruno[7], A. Cappati[7], J. De Favereau De Jeneret[7], C. Delaere[7], A. Giammanco[7], A.O. Guzel[7], V. Lemaitre[7], J. Lidrych[7], P. Malek[7], P. Mastrapasqua[7], S. Turkcapar[7], G.A. Alves[8], M. Barroso Ferreira Filho[8], E. Coelho[8], C. Hensel[8], T. Menezes De Oliveira[8], C. Mora Herrera[222,8], P. Rebello Teles[8], M. Soeiro[8], E.J. Tonelli Manganote[223,8], A. Vilela Pereira[222,8], W.L. Aldá Júnior[9], H. Brandao Malbouisson[9], W. Carvalho[9], J. Chinellato[224,9], M. Costa Reis[9], E.M. Da Costa[9], G.G. Da Silveira[225,9], D. De Jesus Damiao[9], S. Fonseca De Souza[9], R. Gomes De Souza[9], S. S. Jesus[9], T. Laux Kuhn[225,9], M. Macedo[9], K. Mota Amarilo[9], L. Mundim[9], H. Nogima[9], J. P. Pinheiro[9], A. Santoro[9], A. Sznajder[9], M. Thiel[9], F. Torres Da Silva De Araujo[226,9], C. A. Bernardes[225,10], T.R. Fernandez Perez Tomei[10], E.M. Gregores[10], B. Lopes Da Costa[10], I. Maietto Silverio[10], P.G. Mercadante[10], S.F. Novaes[10], B. Orzari[10], Sandra S. Padula[10], V. Scheurer[10], A. Aleksandrov[11], G. Antchev[11], P. Danev[11], R. Hadjiiska[11], P. Iaydjiev[11], M. Misheva[11], M. Shopova[11], G. Sultanov[11], A. Dimitrov[12], L. Litov[12], B. Pavlov[12], P. Petkov[12], A. Petrov[12], S. Keshri[13], D. Laroze[13], S. Thakur[13], W. Brooks[14], T. Cheng[15], T. Javaid[15], L. Wang[15], L. Yuan[15], Z. Hu[16], Z. Liang[16], J. Liu[16], X. Wang[16], G.M. Chen[227,17], H.S. Chen[227,17], M. Chen[227,17], Y. Chen[17], Q. Hou[17], X. Hou[17], C.F. Iemmi[17], H. Jiang[17], A. Kapoor[228,17], H. Liao[17], G. Liu[17], Z.-A. Liu[227,17], J.N. Song[227,17], S. Song[17], J. Tao[17], C. Wang[227,17], J. Wang[17], H. Zhang[17], J. Zhao[17], A. Agapitos[18], Y. Ban[18], A. Carvalho Antunes De Oliveira[18], S. Deng[18], B. Guo[18], Q. Guo[18], C. Jiang[18], A. Levin[18], C. Li[18], Q. Li[18], Y. Mao[18], S. Qian[18], S.J. Qian[18], X. Qin[18], X. Sun[18], D. Wang[18], J. Wang[18], H. Yang[18], M. Zhang[18], Y. Zhao[18], C. Zhou[18], S. Yang[19], Z. You[20], K. Jaffel[21], N. Lu[21], G. Bauer[229,22], B. Li[230,22], H. Wang[22], K. Yi[231,22], J. Zhang[22], Y. Li[23], Z. Lin[24], C. Lu[24], M. Xiao[232,24], C. Avila[25], D.A. Barbosa Trujillo[25], A. Cabrera[25], C. Florez[25], J. Fraga[25], J. A. Reyes Vega[25], C. Rendón[26], M. Rodriguez[26], A.A. Ruales Barbosa[26], J.D. Ruiz Alvarez[26], N. Godinovic[27], D. Lelas[27], A. Sculac[27], M. Kovac[28], A. Petkovic[28], T. Sculac[28], P. Bargassa[29], V. Brigljevic[29], B.K. Chitroda[29], D. Ferencek[29], K. Jakovcic[29], A. Starodumov[29], T. Susa[29], A. Attikis[30], K. Christoforou[30], A. Hadjiagapiou[30], C. Leonidou[30], C. Nicolaou[30], L. Paizanos[30], F. Ptochos[30], P.A. Razis[30], H. Rykaczewski[30], H. Saka[30], A. Stepennov[30], M. Finger[31,218], M. Finger Jr.[31], E. Ayala[32], E. Carrera Jarrin[33], H. Abdalla[233,34], Y. Assran[234,235,34], M. Abdullah Al-Mashad[35], A. Hussein[35], H. Mohammed[35], K. Ehataht[36], M. Kadastik[36], T. Lange[36], C. Nielsen[36], J. Pata[36], M. Raidal[36], N. Seeba[36], L. Tani[36], A. Milieva[37], K. Osterberg[37], M. Voutilainen[37], N. Bin Norjoharuddeen[38], E. Brücken[38], F. Garcia[38], P. Inkaew[38], K.T.S. Kallonen[38], R. Kumar Verma[38], T. Lampén[38], K. Lassila-Perini[38], B. Lehtela[38], S. Lehti[38], T. Lindén[38], N.R. Mancilla Xinto[38], M. Myllymäki[38], M.m. Rantanen[38], S. Saariokari[38], N.T. Toikka[38], J. Tuominiemi[38], H. Kirschenmann[39], P. Luukka[39], H. Petrow[39], M. Besancon[40], F. Couderc[40], M. Dejardin[40], D. Denegri[40], P. Devouge[40], J.L. Faure[40], F. Ferri[40], S. Ganjour[40], P. Gras[40], G. Hamel de Monchenault[40], M. Kumar[40], V. Lohezic[40], J. Malcles[40], F. Orlandi[40], L. Portales[40], S. Ronchi[40], M. Ö. Sahin[40], A. Savoy-Navarro[236,40], P. Simkina[40], M. Titov[40], M. Tornago[40], F. Beaudette[41], G. Boldrini[41], P. Busson[41], C. Charlot[41], M. Chiusi[41], T.D. Cuisset[41], F. Damas[41], O. Davignon[41], A. De Wit[41], T. Debnath[41], I.T. Ehle[41], B.A. Fontana Santos Alves[41], S. Ghosh[41], A. Gilbert[41], R. Granier de Cassagnac[41], L. Kalipoliti[41], M. Manoni[41], M. Nguyen[41], S. Obraztsov[41], C. Ochando[41], R. Salerno[41], J.B. Sauvan[41], Y. Sirois[41], G. Sokmen[41], L. Urda Gómez[41], A. Zabi[41], A. Zghiche[41], J.-L. Agram[237,42], J. Andrea[42], D. Bloch[42], J.-M. Brom[42], E.C. Chabert[42], C. Collard[42], G. Coulon[42], S. Falke[42], U. Goerlach[42], R. Haeberle[42], A.-C. Le Bihan[42], M. Meena[42], O. Poncet[42], G. Saha[42], P. Vaucelle[42], A. Di Florio[43], D. Amram[44], S. Beauceron[44], B. Blancon[44], G. Boudoul[44], N. Chanon[44], D. Contardo[44], P. Depasse[44], C. Dozen[238,44], H. El Mamouni[44], J. Fay[44], S. Gascon[44], M. Gouzevitch[44], C. Greenberg[44], G. Grenier[44], B. Ille[44], E. Jourd'huy[44], I.B. Laktineh[44], M. Lethuillier[44], B. Massoteau[44], L. Mirabito[44], A. Purohit[44], M. Vander Donckt[44], J. Xiao[44], I. Lomidze[45], T. Toriashvili[239,45], Z. Tsamalaidze[240,45], V. Botta[46], S. Consuegra Rodríguez[46], L. Feld[46], K. Klein[46], M. Lipinski[46], D. Meuser[46], P. Nattland[46], V. Oppenländer[46], A. Pauls[46], D. Pérez Adán[46], N. Röwert[46], M. Teroerde[46], C. Daumann[47], S. Diekmann[47], A. Dodonova[47], N. Eich[47], D. Eliseev[47], F. Engelke[47], J. Erdmann[47], M. Erdmann[47], B. Fischer[47], T. Hebbeker[47], K. Hoepfner[47], F. Ivone[47], A. Jung[47], N. Kumar[47], M.y. Lee[47], F. Mausolf[47], M. Merschmeyer[47], A. Meyer[47], F. Nowotny[47], A. Pozdnyakov[47], W. Redjeb[47], H. Reithler[47], U. Sarkar[47], V. Sarkisovi[47], A. Schmidt[47], C. Seth[47], A. Sharma[47], J.L. Spah[47], V. Vaulin[47], S. Zaleski[47], M.R. Beckers[48], C. Dziwok[48], G. Flügge[48], N. Hoeflich[48], T. Kress[48], A. Nowack[48], O. Pooth[48], A. Stahl[48], A. Zotz[48], H. Aarup Petersen[49], A. Abel[49], M. Aldaya Martin[49], J. Alimena[49], S. Amoroso[49], Y. An[49], I. Andreev[49], J. Bach[49], S. Baxter[49], M. Bayatmakou[49], H.Becerril Gonzalez[49], O. Behnke[49], A. Belvedere[49], F. Blekman[241,49], K. Borras[242,49], A. Campbell[49], S. Chatterjee[49], L.X. Coll Saravia[49], G. Eckerlin[49], D. Eckstein[49], E. Gallo[241,49], A. Geiser[49], V. Guglielmi[49], M. Guthoff[49], A. Hinzmann[49], L. Jeppe[49], M. Kasemann[49], C. Kleinwort[49], R. Kogler[49], M. Komm[49], D. Krücker[49], W. Lange[49], D. Leyva Pernia[49], K.-Y. Lin[49], K. Lipka[243,49], W. Lohmann[244,49], J. Malvaso[49], R. Mankel[49], I.-A. Melzer-Pellmann[49], M. Mendizabal Morentin[49], A.B. Meyer[49], G. Milella[49], K. Moral Figueroa[49], A. Mussgiller[49], L.P. Nair[49], J. Niedziela[49], A. Nürnberg[49], J. Park[49], E. Ranken[49], A. Raspereza[49], D. Rastorguev[49], L. Rygaard[49], M. Scham[245,242,49], S. Schnake[242,49], P. Schütze[49], C. Schwanenberger[241,49], D. Selivanova[49], K. Sharko[49], M. Shchedrolosiev[49], D. Stafford[49], M. Torkian[49], F. Vazzoler[49], A. Ventura Barroso[49], R. Walsh[49], D. Wang[49], Q. Wang[49], K. Wichmann[49], L. Wiens[242,49], C. Wissing[49], Y. Yang[49], S. Zakharov[49], A. Zimermmane Castro Santos[49], A. Albrecht[50], A.R. Alves Andrade[50], M. Antonello[50], S. Bollweg[50], M. Bonanomi[50], K. El Morabit[50], Y. Fischer[50], M. Frahm[50], E. Garutti[50], A. Grohsjean[50], A.A. Guvenli[50], J. Haller[50], D. Hundhausen[50], H.R. Jabusch[50], G. Kasieczka[50], P. Keicher[50], R. Klanner[50], W. Korcari[50], T. Kramer[50], C.c. Kuo[50], V. Kutzner[50], F. Labe[50], J. Lange[50], A. Lobanov[50], L. Moureaux[50], M. Mrowietz[50], A. Nigamova[50], K. Nikolopoulos[50], Y. Nissan[50], A. Paasch[50], K.J. Pena Rodriguez[50], N. Prouvost[50], T. Quadfasel[50], B. Raciti[50], M. Rieger[50], D. Savoiu[50], J. Schindler[50], P. Schleper[50], M. Schröder[50], J. Schwandt[50], M. Sommerhalder[50], H. Stadie[50], G. Steinbrück[50], A. Tews[50], R. Ward[50], B. Wiederspan[50], M. Wolf[50], S. Brommer[51], E. Butz[51], Y.M. Chen[51], T. Chwalek[51], A. Dierlamm[51], G.G. Dincer[51], U. Elicabuk[51], N. Faltermann[51], M. Giffels[51], A. Gottmann[51], F. Hartmann[246,51], R. Hofsaess[51], M. Horzela[51], U. Husemann[51], J. Kieseler[51], M. Klute[51], R. Kunnilan Muhammed Rafeek[51], O. Lavoryk[51], J.M. Lawhorn[51], A. Lintuluoto[51], S. Maier[51], M. Mormile[51], Th. Müller[51], E.

Pfeffer[51], M. Presilla[51], G. Quast[51], K. Rabbertz[51], B. Regnery[51], R. Schmieder[51], N. Shadskiy[51], I. Shvetsov[51], H.J. Simonis[51], L. Sowa[51], L. Stockmeier[51], K. Tauqeer[51], M. Toms[51], B. Topko[51], N. Trevisani[51], C. Verstege[51], T. Voigtländer[51], R.F. Von Cube[51], J. Von Den Driesch[51], M. Wassmer[51], R. Wolf[51], W.D. Zeuner[51], X. Zuo[51], G. Anagnostou[52], G. Daskalakis[52], A. Kyriakis[52], A. Papadopoulos[246,52], A. Stakia[52], G. Melachroinos[53], Z. Painesis[53], I. Paraskevas[53], N. Saoulidou[53], K. Theofilatos[53], E. Tziaferi[53], K. Vellidis[53], I. Zisopoulos[53], T. Chatzistavrou[54], G. Karapostoli[54], K. Kousouris[54], E. Siamarkou[54], G. Tsipolitis[54], I. Bestintzanos[55], I. Evangelou[55], C. Foudas[55], P. Katsoulis[55], P. Kokkas[55], P.G. Kosmoglou Kioseoglou[55], N. Manthos[55], I. Papadopoulos[55], J. Strologas[55], D. Druzhkin[56], C. Hajdu[56], D. Horvath[247,248,56], K. Márton[56], A.J. Rádl[249,56], F. Sikler[56], V. Veszpremi[56], M. Csanád[57], K. Farkas[57], A. Fehérkuti[250,57], M.M.A. Gadallah[251,57], Á. Kadlecsik[57], M. León Coello[57], G. Pásztor[57], G.I. Veres[57], B. Ujvari[58], G. Zilizi[58], G. Bencze[59], S. Czellar[59], J. Molnar[59], Z. Szillasi[59], T. Csorgo[250,60], F. Nemes[250,60], T. Novak[60], I. Szanyi[252,60], S. Bansal[61], S.B. Beri[61], V. Bhatnagar[61], G. Chaudhary[61], S. Chauhan[61], N. Dhingra[253,61], A. Kaur[61], A. Kaur[61], H. Kaur[61], M. Kaur[61], S. Kumar[61], T. Sheokand[61], J.B. Singh[61], A. Singla[61], A. Bhardwaj[62], A. Chhetri[62], B.C. Choudhary[62], A. Kumar[62], A. Kumar[62], M. Naimuddin[62], S. Phor[62], K. Ranjan[62], M.K. Saini[62], S. Acharya[254,63], B. Gomber[254,63], B. Sahu[254,63], S. Mukherjee[64], S. Baradia[65], S. Bhattacharya[65], S. Das Gupta[65], S. Dutta[65], S. Dutta[65], S. Sarkar[65], M.M. Ameen[66], P.K. Behera[66], S. Chatterjee[66], G. Dash[66], A. Dattamunsi[66], P. Jana[66], P. Kalbhor[66], S. Kamble[66], J.R. Komaragiri[255,66], T. Mishra[66], P.R. Pujahari[66], N.R. Saha[66], A.K. Sikdar[66], R.K. Singh[66], P. Verma[66], S. Verma[66], A. Vijay[66], B.K. Sirasva[67], L. Bhatt[68], S. Dugad[68], G.B. Mohanty[68], M. Shelake[68], P. Suryadevara[68], A. Bala[69], S. Banerjee[69], S. Barman[256,69], R.M. Chatterjee[69], M. Guchait[69], Sh. Jain[69], A. Jaiswal[69], B.M. Joshi[69], S. Kumar[69], M. Maity[256,69], G. Majumder[69], K. Mazumdar[69], S. Parolia[69], R. Saxena[69], A. Thachayath[69], S. Bahinipati[257,70], D. Maity[258,70], P. Mal[70], K. Naskar[258,70], A. Nayak[258,70], S. Nayak[70], K. Pal[70], R. Raturi[70], P. Sadangi[70], S.K. Swain[70], S. Varghese[258,70], D. Vats[258,70], A. Alpana[71], S. Dube[71], P. Hazarika[71], B. Kansal[71], A. Laha[71], R. Sharma[71], S. Sharma[71], K.Y. Vaish[71], S. Ghosh[72], H. Bakhshiansohi[259,73], A. Jafari[260,73], V. Sedighzadeh Dalavi[73], M. Zeinali[261,73], S. Bashiri[74], S. Chenarani[262,74], S.M. Etesami[74], Y. Hosseini[74], M. Khakzad[74], E. Khazaie[74], M. Mohammadi Najafabadi[74], S. Tizchang[263,74], M. Felcini[75], M. Grunewald[75], M. Abbrescia[76,77], M. Barbieri[76,77], M. Buonsante[76,77], A. Colaleo[76,77], D. Creanza[76,78], B. D'Anzi[76,77], N. De Filippis[76,78], M. De Palma[76,77], W. Elmetenawee[264,76,77], N. Ferrara[76,78], L. Fiore[76], L. Longo[76], M. Louka[76,77], G. Maggi[76,78], M. Maggi[76], I. Margjeka[76], V. Mastrapasqua[76,77], S. My[76,77], F. Nenna[76,77], S. Nuzzo[76,77], A. Pellecchia[76,77], A. Pompili[76,77], G. Pugliese[76,78], R. Radogna[76,77], D. Ramos[76,77], A. Ranieri[76], L. Silvestris[76], F.M. Simone[76,78], Ü. Sözbilir[76], A. Stamerra[76,77], D. Troiano[76,77], R. Venditti[76,77], P. Verwilligen[76], A. Zaza[76,77], G. Abbiendi[79], C. Battilana[79,80], D. Bonacorsi[79,80], P. Capiluppi[79,80], M. Cuffiani[79,80], G.M. Dallavalle[79], T. Diotalevi[79,80], F. Fabbri[79], A. Fanfani[79,80], D. Fasanella[79], P. Giacomelli[79], C. Grandi[79], L. Guiducci[79,80], S. Lo Meo[265,79], M. Lorusso[79,80], L. Lunerti[79], S. Marcellini[79], G. Masetti[79], F.L. Navarria[79,80], G. Paggi[79,80], A. Perrotta[79], F. Primavera[79,80], A.M. Rossi[79,80], S. Rossi Tisbeni[79,80], T. Rovelli[79,80], G.P. Siroli[79,80], S. Costa[266,81,82], A. Di Mattia[81], A. Lapertosa[81], R. Potenza[81,82], A. Tricomi[266,81,82], J. Altork[83,84], P. Assiouras[83], G. Barbagli[83], G. Bardelli[83], M. Bartolini[83,84], A. Calandri[83,84], B. Camaiani[83,84], A. Cassese[83], R. Ceccarelli[83], V. Ciulli[83,84], C. Civinini[83], R. D'Alessandro[83,84], L. Damenti[83,84], E. Focardi[83,84], T. Kello[83], G. Latino[83,84], P. Lenzi[83,84], M. Lizzo[83], M. Meschini[83], S. Paoletti[83], A. Papanastassiou[83,84], G. Sguazzoni[83], L. Viliani[83], L. Benussi[85], S. Colafranceschi[85], S. Meola[267,85], D. Piccolo[85], M. Alves Gallo Pereira[86], F. Ferro[86], E. Robutti[86], S. Tosi[86,87], A. Benaglia[88], F. Brivio[88], V. Camagni[88,89], F. Cetorelli[88,89], F. De Guio[88,89], M.E. Dinardo[88,89], P. Dini[88], S. Gennai[88], R. Gerosa[88,89], A. Ghezzi[88,89], P. Govoni[88,89], L. Guzzi[88], M.R. Kim[88], G. Lavizzari[88,89], M.T. Lucchini[88,89], M. Malberti[88], S. Malvezzi[88], A. Massironi[88], D. Menasce[88], L. Moroni[88], M. Paganoni[88,89], S. Palluotto[88,89], D. Pedrini[88], A. Perego[88,89], B.S. Pinolini[88], G. Pizzati[88,89], S. Ragazzi[88,89], T. Tabarelli de Fatis[88,89], S. Buontempo[90], A. Cagnotta[90,91], C. Di Fraia[90,91], F. Fabozzi[90,92], L. Favilla[90,93], A.O.M. Iorio[90,91], L. Lista[268,90,91], P. Paolucci[246,90], B. Rossi[90], P. Azzi[94], N. Bacchetta[269,94], D. Bisello[94,95], P. Bortignon[94], G. Bortolato[94,95], A.C.M. Bulla[94], R. Carlin[94,95], T. Dorigo[270,94], F. Gasparini[94,95], S. Giorgetti[94], A. Gozzelino[94], E. Lusiani[94], M. Margoni[94,95], A.T. Meneguzzo[94,95], J. Pazzini[94,95], P. Ronchese[94,95], R. Rossin[94,95], F. Simonetto[94,95], M. Tosi[94,95], A. Triossi[94,95], S. Ventura[94], M. Zanetti[94,95], P. Zotto[94,95], A. Zucchetta[94,95], G. Zumerle[94,95], A. Braghieri[97], S. Calzaferri[97], P. Montagna[97,98], M. Pelliccioni[97], V. Re[97], C. Riccardi[97,98], P. Salvini[97], I. Vai[97,98], P. Vitulo[97,98], S. Ajmal[99,100], M.E. Ascioti[99,100], G.M. Bilei[99], C. Carrivale[99,100], D. Ciangottini[99,100], L. Della Penna[99,100], L. Fanò[99,100], V. Mariani[99,100], M. Menichelli[99], F. Moscatelli[271,99], A. Rossi[99,100], A. Santocchia[99,100], D. Spiga[99], T. Tedeschi[99,100], C. Aimè[101,102], C.A. Alexe[101,102], P. Asenov[101,102], P. Azzurri[101], G. Bagliesi[101], R. Bhattacharya[101], L. Bianchini[101,102], T. Boccali[101], E. Bossini[101], D. Bruschini[101,103], L. Calligaris[101,102], R. Castaldi[101], F. Cattafesta[101,103], M.A. Ciocci[101,104], M. Cipriani[101,102], V. D'Amante[101,104], R. Dell'Orso[101], S. Donato[101,102], R. Forti[101,102], A. Giassi[101], F. Ligabue[101,103], A.C. Marini[101,102], D. Matos Figueiredo[101], A. Messineo[101,102], S. Mishra[101], V.K. Muraleedharan Nair Bindhu[101,102], S. Nandan[101], F. Palla[101], M. Riggirello[101,103], A. Rizzi[101,102], G. Rolandi[101,103], S. Roy Chowdhury[272,101], T. Sarkar[101], A. Scribano[101], P. Solanki[101,102], P. Spagnolo[101], F. Tenchini[101,102], R. Tenchini[101], G. Tonelli[101,102], N. Turini[101,104], F. Vaselli[101,103], A. Venturi[101], P.G. Verdini[101], P. Akrap[105,106], C. Basile[105,106], S.C. Behera[105], F. Cavallari[105], L. Cunqueiro Mendez[105,106], F. De Riggi[105,106], D. Del Re[105,106], E. Di Marco[105], M. Diemoz[105], F. Errico[105], L. Frosina[105,106], R. Gargiulo[105,106], B. Harikrishnan[105,106], F. Lombardi[105,106], E. Longo[105,106], L. Martikainen[105,106], J. Mijuskovic[105,106], G. Organtini[105,106], N. Palmeri[105,106], R. Paramatti[105,106], C. Quaranta[105,106], S. Rahatlou[105,106], C. Rovelli[105], F. Santanastasio[105,106], L. Soffi[105], V. Vladimirov[105,106], N. Amapane[107,108], R. Arcidiacono[107,109], S. Argiro[107,108], M. Arneodo[107,109], N. Bartosik[107,109], R. Bellan[107,108], A. Bellora[107,108], C. Biino[107], C. Borca[107,108], N. Cartiglia[107], M. Costa[107,108], R. Covarelli[107,108], N. Demaria[107], L. Finco[107], M. Grippo[107,108], B. Kiani[107,108], F. Legger[107], F. Luongo[107,108], C. Mariotti[107], S. Maselli[107], A. Mecca[107,108], L. Menzio[107,108], P. Meridiani[107], E. Migliore[107,108], M. Monteno[107], M.M. Obertino[107,108], G. Ortona[107], L. Pacher[107,108], N. Pastrone[107], M. Ruspa[107,109], F. Siviero[107,108], V. Sola[107,108], A. Solano[107,108], A. Staiano[107], C. Tarricone[107,108], D. Trocino[107], G. Umoret[107,108], E. Vlasov[107,108], R. White[107,108], J. Babbar[110,111], S. Belforte[110], V. Candelise[110,111], M. Casarsa[110], F. Cossutti[110], K. De Leo[110], G. Della Ricca[110,111], R. Delli Gatti[110,111], S. Dogra[112], J. Hong[112], J. Kim[112], T. Kim[112], D. Lee[112], H. Lee[112], J. Lee[112], S.W. Lee[112], C.S. Moon[112], Y.D. Oh[112], S. Sekmen[112], B. Tae[112], Y.C. Yang[112], M.S. Kim[113], G. Bak[114], P. Gwak[114], H. Kim[114], D.H. Moon[114], J. Seo[114], E. Asilar[115], F. Carnevali[115], J. Choi[273,115], T.J. Kim[115], Y. Ryou[115], S. Ha[116], S. Han[116], B. Hong[116], K. Lee[116], K.S. Lee[116], S. Lee[116], J. Yoo[116], J. Goh[117], J. Shin[117], S. Yang[117], Y. Kang[118], H. S. Kim[118], Y. Kim[118], S. Lee[118], J. Almond[119], J.H. Bhyun[119], J. Choi[119], J. Choi[119], W. Jun[119], H. Kim[119], J. Kim[119], T. Kim[119], Y. Kim[119], Y.W. Kim[119], S. Ko[119], H. Lee[119], J. Lee[119], J. Lee[119], B.H. Oh[119], S.B. Oh[119], J.

Shin[119], U.K. Yang[119], I. Yoon[119], W. Jang[120], D.Y. Kang[120], D. Kim[120], S. Kim[120], B. Ko[120], J.S.H. Lee[120], Y. Lee[120], J.A. Merlin[120], I.C. Park[120], Y. Roh[120], I.J. Watson[120], G. Cho[121], K. Hwang[121], B. Kim[121], S. Kim[121], K. Lee[121], H.D. Yoo[121], M. Choi[122], Y. Lee[122], I. Yu[122], T. Beyrouthy[123], Y. Gharbia[123], F. Alazemi[124], K. Dreimanis[125], O.M. Eberlins[125], A. Gaile[125], C. Munoz Diaz[125], D. Osite[125], G. Pikurs[125], R. Plese[125], A. Potrebko[125], M. Seidel[125], D. Sidiropoulos Kontos[125], N.R. Strautnieks[126], M. Ambrozas[127], A. Juodagalvis[127], S. Nargelas[127], A. Rinkevicius[127], G. Tamulaitis[127], I. Yusuff[274,128], Z. Zolkapli[128], J.F. Benitez[129], A. Castaneda Hernandez[129], A. Cota Rodriguez[129], L.E. Cuevas Picos[129], H.A. Encinas Acosta[129], L.G. Gallegos Maríñez[129], J.A. Murillo Quijada[129], A. Sehrawat[129], L. Valencia Palomo[129], G. Ayala[130], H. Castilla-Valdez[130], H. Crotte Ledesma[130], R. Lopez-Fernandez[130], J. Mejia Guisao[130], R. Reyes-Almanza[130], A. Sánchez Hernández[130], C. Oropeza Barrera[131], D.L. Ramirez Guadarrama[131], M. Ramírez García[131], I. Bautista[132], F.E. Neri Huerta[132], I. Pedraza[132], H.A. Salazar Ibarguen[132], C. Uribe Estrada[132], I. Bubanja[133], N. Raicevic[133], P.H. Butler[134], A. Ahmad[135], M.I. Asghar[135], A. Awais[135], M.I.M. Awan[135], W.A. Khan[135], V. Avati[136], L. Forthomme[136], L. Grzanka[136], M. Malawski[136], K. Piotrzkowski[136], M. Bluj[137], M. Górski[137], M. Kazana[137], M. Szleper[137], P. Zalewski[137], K. Bunkowski[138], K. Doroba[138], A. Kalinowski[138], M. Konecki[138], J. Krolikowski[138], A. Muhammad[138], P. Fokow[139], K. Pozniak[139], W. Zabolotny[139], M. Araujo[140], D. Bastos[140], C. Beirão Da Cruz E Silva[140], A. Boletti[140], M. Bozzo[140], T. Camporesi[140], G. Da Molin[140], P. Faccioli[140], M. Gallinaro[140], J. Hollar[140], N. Leonardo[140], G.B. Marozzo[140], A. Petrilli[140], M. Pisano[140], J. Seixas[140], J. Varela[140], J.W. Wulff[140], P. Adzic[141], L. Markovic[141], P. Milenovic[141], V. Milosevic[141], D. Devetak[142], M. Dordevic[142], J. Milosevic[142], L. Nadderd[142], V. Rekovic[142], M. Stojanovic[142], M. Alcalde Martinez[143], J. Alcaraz Maestre[143], Cristina F. Bedoya[143], J.A. Brochero Cifuentes[143], Oliver M. Carretero[143], M. Cepeda[143], M. Cerrada[143], N. Colino[143], J. Cuchillo Ortega[143], B. De La Cruz[143], A. Delgado Peris[143], A. Escalante Del Valle[143], D. Fernández Del Val[143], J.P. Fernández Ramos[143], J. Flix[143], M.C. Fouz[143], M. Gonzalez Hernandez[143], O. Gonzalez Lopez[143], S. Goy Lopez[143], J.M. Hernandez[143], M.I. Josa[143], J. Llorente Merino[143], C. Martin Perez[143], E. Martin Viscasillas[143], D. Moran[143], C. M. Morcillo Perez[143], R. Paz Herrera[143], C. Perez Dengra[143], A. Pérez-Calero Yzquierdo[143], J. Puerta Pelayo[143], I. Redondo[143], J. Vazquez Escobar[143], J.F. de Trocóniz[144], B. Alvarez Gonzalez[145], J. Ayllon Torresano[145], A. Cardini[145], J. Cuevas[145], J. Del Riego Badas[145], D. Estrada Acevedo[145], J. Fernandez Menendez[145], S. Folgueras[145], I. Gonzalez Caballero[145], P. Leguina[145], M. Obeso Menendez[145], E. Palencia Cortezon[145], J. Prado Pico[145], A. Soto Rodríguez[145], C. Vico Villalba[145], P. Vischia[145], S. Blanco Fernández[146], I.J. Cabrillo[146], A. Calderon[146], J. Duarte Campderros[146], M. Fernandez[146], G. Gomez[146], C. Lasaosa García[146], R. Lopez Ruiz[146], C. Martinez Rivero[146], P. Martinez Ruiz del Arbol[146], F. Matorras[146], P. Matorras Cuevas[146], E. Navarrete Ramos[146], J. Piedra Gomez[146], C. Quintana San Emeterio[146], L. Scodellaro[146], I. Vila[146], R. Vilar Cortabitarte[146], J.M. Vizan Garcia[146], B. Kailasapathy[275,147], D.D.C. Wickramarathna[147], W.G.D. Dharmaratna[276,148], K. Liyanage[148], N. Perera[148], D. Abbaneo[149], C. Amendola[149], R. Ardino[149], E. Auffray[149], J. Baechler[149], D. Barney[149], M. Bianco[149], A. Bocci[149], L. Borgonovi[149], C. Botta[149], A. Bragagnolo[149], C.E. Brown[149], C. Caillol[149], G. Cerminara[149], P. Connor[149], D. d'Enterria[149], A. Dabrowski[149], A. David[149], A. De Roeck[149], M.M. Defranchis[149], M. Deile[149], M. Dobson[149], W. Funk[149], A. Gaddi[149], S. Giani[149], D. Gigi[149], K. Gill[149], F. Glege[149], M. Glowacki[149], A. Gruber[149], J. Hegeman[149], J.K. Heikkilä[149], B. Huber[149], V. Innocente[149], T. James[149], P. Janot[149], O. Kaluzinska[149], O. Karacheban[244,149], G. Karathanasis[149], L. Lanteri[149], S. Laurila[149], P. Lecoq[149], C. Lourenço[149], A.-M. Lyon[149], M. Magherini[149], L. Malgeri[149], M. Mannelli[149], A. Mehta[149], F. Meijers[149], S. Mersi[149], E. Meschi[149], M. Migliorini[149], F. Monti[149], F. Moortgat[149], M. Mulders[149], M. Musich[149], I. Neutelings[149], S. Orfanelli[149], F. Pantaleo[149], M. Pari[149], G. Petrucciani[149], A. Pfeiffer[149], M. Pierini[149], M. Pitt[149], H. Qu[149], D. Rabady[149], B. Ribeiro Lopes[149], F. Riti[149], P. Rosado[149], M. Rovere[149], H. Sakulin[149], R. Salvatico[149], S. Sanchez Cruz[149], S. Scarfi[149], M. Selvaggi[149], A. Sharma[149], K. Shchelina[149], P. Silva[149], P. Sphicas[277,149], A.G. Stahl Leiton[149], A. Steen[149], S. Summers[149], D. Treille[149], P. Tropea[149], E. Vernazza[149], J. Wanczyk[278,149], J. Wang[149], S. Wuchterl[149], M. Zarucki[149], P. Zehetner[149], P. Zejdl[149], G. Zevi Della Porta[149], T. Bevilacqua[279,150], L. Caminada[279,150], W. Erdmann[150], R. Horisberger[150], Q. Ingram[150], H.C. Kaestli[150], D. Kotlinski[150], C. Lange[150], U. Langenegger[150], M. Missiroli[279,150], L. Noehte[279,150], T. Rohe[150], A. Samalan[150], T.K. Aarrestad[151], M. Backhaus[151], G. Bonomelli[151], C. Cazzaniga[151], K. Datta[151], P. De Bryas Dexmiers D'archiacchiac[278,151], A. De Cosa[151], G. Dissertori[151], M. Dittmar[151], M. Donegà[151], F. Eble[151], K. Gedia[151], F. Glessgen[151], C. Grab[151], N. Härringer[151], T.G. Harte[151], W. Lustermann[151], M. Malucchi[151], R.A. Manzoni[151], M. Marchegiani[151], L. Marchese[151], A. Mascellani[278,151], F. Nessi-Tedaldi[151], F. Pauss[151], V. Perovic[151], B. Ristic[151], R. Seidita[151], J. Steggemann[278,151], A. Tarabini[151], D. Valsecchi[151], R. Wallny[151], C. Amsler[280,152], P. Bärtschi[152], F. Bilandzija[152], M.F. Canelli[152], G. Celotto[152], K. Cormier[152], M. Huwiler[152], W. Jin[152], A. Jofrehei[152], B. Kilminster[152], T.H. Kwok[152], S. Leontsinis[152], V. Lukashenko[152], A. Macchiolo[152], F. Meng[152], J. Motta[152], A. Reimers[152], P. Robmann[152], M. Senger[152], E. Shokr[152], F. Stäger[152], R. Tramontano[152], D. Bhowmik[153], C.M. Kuo[153], P.K. Rout[153], S. Taj[153], P.C. Tiwari[255,153], L. Ceard[154], K.F. Chen[154], Z.g. Chen[154], A. De Iorio[154], W.-S. Hou[154], T.h. Hsu[154], Y.w. Kao[154], S. Karmakar[154], G. Kole[154], Y.y. Li[154], R.-S. Lu[154], E. Paganis[154], X.f. Su[154], J. Thomas-Wilsker[154], L.s. Tsai[154], D. Tsionou[154], H.y. Wu[154], E. Yazgan[154], C. Asawatangtrakuldee[155], N. Srimanobhas[155], Y. Maghrbi[156], D. Agyel[157], F. Dolek[157], I. Dumanoglu[281,157], Y. Guler[282,157], E. Gurpinar Guler[282,157], C. Isik[157], O. Kara[157], A. Kayis Topaksu[157], Y. Komurcu[157], G. Onengut[157], K. Ozdemir[283,157], B. Tali[284,157], U.G. Tok[157], E. Uslan[157], I.S. Zorbakir[157], M. Yalvac[285,158], B. Akgun[159], I.O. Atakisi[286,159], E. Gülmez[159], M. Kaya[287,159], O. Kaya[288,159], M.A. Sarkisla[289,159], S. Tekten[290,159], A. Cakir[160], K. Cankocak[281,291,160], S. Sen[292,160], O. Aydilek[293,161], B. Hacisahinoglu[161], I. Hos[294,161], B. Kaynak[161], S. Ozkorucuklu[161], O. Potok[161], H. Sert[161], C. Simsek[161], C. Zorbilmez[161], S. Cerci[162], B. Isildak[295,162], D. Sunar Cerci[162], T. Yetkin[238,162], A. Boyaryntsev[163], O. Dadazhanova[163], B. Grynyov[163], L. Levchuk[164], J.J. Brooke[165], A. Bundock[165], F. Bury[165], E. Clement[165], D. Cussans[165], D. Dharmender[165], H. Flacher[165], J. Goldstein[165], H.F. Heath[165], M.-L. Holmberg[165], L. Kreczko[165], S. Paramesvaran[165], L. Robertshaw[165], M.S. Sanjrani[165], J. Segal[165], V.J. Smith[165], A.H. Ball[166], K.W. Bell[166], A. Belyaev[296,166], C. Brew[166], R.M. Brown[166], D.J.A. Cockerill[166], C. Cooke[166], A. Elliot[166], K.V. Ellis[166], J. Gajownik[166], K. Harder[166], S. Harper[166], J. Linacre[166], K. Manolopoulos[166], M. Moallemi[166], D.M. Newbold[166], E. Olaiya[166], D. Petyt[166], T. Reis[166], A.R. Sahasransu[166], G. Salvi[166], T. Schuh[166], C.H. Shepherd-Themistocleous[166], I.R. Tomalin[166], K.C. Whalen[166], T. Williams[166], I. Andreou[167], R. Bainbridge[167], P. Bloch[167], O. Buchmuller[167], C.A. Carrillo Montoya[167], D. Colling[167], J.S. Dancu[167], I. Das[167], P. Dauncey[167], G. Davies[167], M. Della Negra[167], S. Fayer[167], G. Fedi[167], G. Hall[167], H.R. Hoorani[167], A. Howard[167], G. Iles[167], C.R. Knight[167], P. Krueper[167], J. Langford[167], K.H. Law[167], J. León Holgado[167], E. Leutgeb[167], L. Lyons[167], A.-M. Magnan[167], B. Maier[167], S. Mallios[167], A. Mastronikolis[167], M. Mieskolainen[167],

J. Nash[297,167], M. Pesaresi[167], P.B. Pradeep[167], B.C. Radburn-Smith[167], A. Richards[167], A. Rose[167], L. Russell[167], K. Savva[167], C. Seez[167], R. Shukla[167], A. Tapper[167], K. Uchida[167], G.P. Uttley[167], T. Virdee[246,167], M. Vojinovic[167], N. Wardle[167], D. Winterbottom[167], J.E. Cole[168], A. Khan[168], P. Kyberd[168], I.D. Reid[168], S. Abdullin[169], A. Brinkerhoff[169], E. Collins[169], M.R. Darwish[169], J. Dittmann[169], K. Hatakeyama[169], V. Hegde[169], J. Hiltbrand[169], B. McMaster[169], J. Samudio[169], S. Sawant[169], C. Sutantawibul[169], J. Wilson[169], J.M. Hogan[298,170], R. Bartek[171], A. Dominguez[171], S. Raj[171], A.E. Simsek[171], S.S. Yu[171], B. Bam[172], A. Buchot Perraguin[172], S. Campbell[172], R. Chudasama[172], S.I. Cooper[172], C. Crovella[172], G. Fidalgo[172], S.V. Gleyzer[172], A. Khukhunaishvili[172], K. Matchev[172], E. Pearson[172], C.U. Perez[172], P. Rumerio[299,172], E. Usai[172], R. Yi[172], S. Cholak[173], G. De Castro[173], Z. Demiragli[173], C. Erice[173], C. Fangmeier[173], C. Fernandez Madrazo[173], E. Fontanesi[173], J. Fulcher[173], F. Golf[173], S. Jeon[173], J. O'Cain[173], I. Reed[173], J. Rohlf[173], K. Salyer[173], D. Sperka[173], D. Spitzbart[173], I. Suarez[173], A. Tsatsos[173], E. Wurtz[173], A.G. Zecchinelli[173], G. Barone[174], G. Benelli[174], D. Cutts[174], S. Ellis[174], L. Gouskos[174], M. Hadley[174], U. Heintz[174], K.W. Ho[174], T. Kwon[174], G. Landsberg[174], K.T. Lau[174], J. Luo[174], S. Mondal[174], J. Roloff[174], T. Russell[174], S. Sagir[300,174], X. Shen[174], M. Stamenkovic[174], N. Venkatasubramanian[174], S. Abbott[175], B. Barton[175], R. Breedon[175], H. Cai[175], M. Calderon De La Barca Sanchez[175], M. Chertok[175], M. Citron[175], J. Conway[175], P.T. Cox[175], R. Erbacher[175], O. Kukral[175], G. Mocellin[175], S. Ostrom[175], W. Wei[175], S. Yoo[175], K. Adamidis[176], M. Bachtis[176], D. Campos[176], R. Cousins[176], A. Datta[176], G. Flores Avila[176], J. Hauser[176], M. Ignatenko[176], M.A. Iqbal[176], T. Lam[176], Y.f. Lo[176], E. Manca[176], A. Nunez Del Prado[176], D. Saltzberg[176], V. Valuev[176], R. Clare[177], J.W. Gary[177], G. Hanson[177], A. Aportela[178], A. Arora[178], J.G. Branson[178], S. Cittolin[178], S. Cooperstein[178], D. Diaz[178], J. Duarte[178], L. Giannini[178], Y. Gu[178], J. Guiang[178], V. Krutelyov[178], R. Lee[178], J. Letts[178], H. Li[178], M. Masciovecchio[178], F. Mokhtar[178], S. Mukherjee[178], M. Pieri[178], D. Primosch[178], M. Quinnan[178], V. Sharma[178], M. Tadel[178], E. Vourliotis[178], F. Würthwein[178], A. Yagil[178], Z. Zhao[178], A. Barzdukas[179], L. Brennan[179], C. Campagnari[179], S. Carron Montero[301,179], K. Downham[179], C. Grieco[179], M.M. Hussain[179], J. Incandela[179], J. Kim[179], M.W.K. Lai[179], A.J. Li[179], P. Masterson[179], J. Richman[179], S.N. Santpur[179], U. Sarica[179], R. Schmitz[179], F. Setti[179], J. Sheplock[179], D. Stuart[179], T.Á. Vámi[179], X. Yan[179], D. Zhang[179], A. Albert[180], S. Bhattacharya[180], A. Bornheim[180], O. Cerri[180], R. Kansal[180], J. Mao[180], H.B. Newman[180], G. Reales Gutiérrez[180], T. Sievert[180], M. Spiropulu[180], J.R. Vlimant[180], R.A. Wynne[180], S. Xie[180], J. Alison[181], S. An[181], M. Cremonesi[181], V. Dutta[181], E.Y. Ertorer[181], T. Ferguson[181], T.A. Gómez Espinosa[181], A. Harilal[181], A. Kallil Tharayil[181], M. Kanemura[181], C. Liu[181], P. Meiring[181], T. Mudholkar[181], S. Murthy[181], P. Palit[181], K. Park[181], M. Paulini[181], A. Roberts[181], A. Sanchez[181], W. Terrill[181], J.P. Cumalat[182], W.T. Ford[182], A. Hart[182], A. Hassani[182], S. Kwan[182], J. Pearkes[182], C. Savard[182], N. Schonbeck[182], K. Stenson[182], K.A. Ulmer[182], S.R. Wagner[182], N. Zipper[182], D. Zuolo[182], J. Alexander[183], X. Chen[183], D.J. Cranshaw[183], J. Dickinson[183], J. Fan[183], X. Fan[183], J. Grassi[183], S. Hogan[183], P. Kotamnives[183], J. Monroy[183], G. Niendorf[183], M. Oshiro[183], J.R. Patterson[183], M. Reid[183], A. Ryd[183], J. Thom[183], P. Wittich[183], R. Zou[183], L. Zygala[183], M. Albrow[184], M. Alyari[184], O. Amram[184], G. Apollinari[184], A. Apresyan[184], L.A.T. Bauerdick[184], D. Berry[184], J. Berryhill[184], P.C. Bhat[184], K. Burkett[184], J.N. Butler[184], A. Canepa[184], G.B. Cerati[184], H.W.K. Cheung[184], F. Chlebana[184], C. Cosby[184], G. Cummings[184], I. Dutta[184], V.D. Elvira[184], J. Freeman[184], A. Gandrakota[184], Z. Gecse[184], L. Gray[184], D. Green[184], A. Grummer[184], S. Grünendahl[184], D. Guerrero[184], O. Gutsche[184], R.M. Harris[184], T.C. Herwig[184], J. Hirschauer[184], B. Jayatilaka[184], S. Jindariani[184], M. Johnson[184], U. Joshi[184], T. Klijnsma[184], B. Klima[184], K.H.M. Kwok[184], S. Lammel[184], C. Lee[184], D. Lincoln[184], R. Lipton[184], T. Liu[184], K. Maeshima[184], D. Mason[184], P. McBride[184], P. Merkel[184], S. Mrenna[184], S. Nahn[184], J. Ngadiuba[184], D. Noonan[184], S. Norberg[184], V. Papadimitriou[184], N. Pastika[184], K. Pedro[184], C. Pena[302,184], C.E. Perez Lara[184], F. Ravera[184], A. Reinsvold Hall[303,184], L. Ristori[184], M. Safdari[184], E. Sexton-Kennedy[184], N. Smith[184], A. Soha[184], L. Spiegel[184], S. Stoynev[184], J. Strait[184], L. Taylor[184], S. Tkaczyk[184], N.V. Tran[184], L. Uplegger[184], E.W. Vaandering[184], C. Wang[184], I. Zoi[184], C. Aruta[185], P. Avery[185], D. Bourilkov[185], P. Chang[185], V. Cherepanov[185], R.D. Field[185], C. Huh[185], E. Koenig[185], M. Kolosova[185], J. Konigsberg[185], A. Korytov[185], N. Menendez[185], G. Mitselmakher[185], K. Mohrman[185], A. Muthirakalayil Madhu[185], N. Rawal[185], S. Rosenzweig[185], V. Sulimov[185], Y. Takahashi[185], J. Wang[185], T. Adams[186], A. Al Kadhim[186], A. Askew[186], S. Bower[186], R. Hashmi[186], R.S. Kim[186], T. Kolberg[186], G. Martinez[186], M. Mazza[186], H. Prosper[186], P.R. Prova[186], M. Wulansatiti[186], R. Yohay[186], B. Alsufyani[187], S. Butalla[187], S. Das[187], M. Hohlmann[187], M. Lavinsky[187], E. Yanes[187], M.R. Adams[188], N. Barnett[188], A. Baty[188], C. Bennett[188], R. Cavanaugh[188], R. Escobar Franco[188], O. Evdokimov[188], C.E. Gerber[188], H. Gupta[188], M. Hawksworth[188], A. Hingrajiya[188], D.J. Hofman[188], J.h. Lee[188], D. S. Lemos[188], C. Mills[188], S. Nanda[188], G. Nigmatkulov[188], B. Ozek[188], T. Phan[188], D. Pilipovic[188], R. Pradhan[188], E. Prifti[188], P. Roy[188], T. Roy[188], N. Singh[188], M.B. Tonjes[188], N. Varelas[188], M.A. Wadud[188], J. Yoo[188], M. Alhusseini[189], D. Blend[189], K. Dilsiz[304,189], O.K. Köseyan[189], A. Mestvirishvili[305,189], O. Neogi[189], H. Ogul[306,189], Y. Onel[189], A. Penzo[189], C. Snyder[189], E. Tiras[307,189], B. Blumenfeld[190], J. Davis[190], A.V. Gritsan[190], L. Kang[190], S. Kyriacou[190], P. Maksimovic[190], M. Roguljic[190], S. Sekhar[190], M.V. Srivastav[190], M. Swartz[190], A. Abreu[191], L.F. Alcerro Alcerro[191], J. Anguiano[191], S. Arteaga Escatel[191], P. Baringer[191], A. Bean[191], Z. Flowers[191], D. Grove[191], J. King[191], G. Krintiras[191], M. Lazarovits[191], C. Le Mahieu[191], J. Marquez[191], M. Murray[191], M. Nickel[191], S. Popescu[308,191], C. Rogan[191], C. Royon[191], S. Rudrabhatla[191], S. Sanders[191], C. Smith[191], G. Wilson[191], B. Allmond[192], R. Gujju Gurunadha[192], N. Islam[192], A. Ivanov[192], K. Kaadze[192], Y. Maravin[192], J. Natoli[192], D. Roy[192], G. Sorrentino[192], A. Baden[193], A. Belloni[193], J. Bistany-riebman[193], S.C. Eno[193], N.J. Hadley[193], S. Jabeen[193], R.G. Kellogg[193], T. Koeth[193], B. Kronheim[193], S. Lascio[193], P. Major[193], A.C. Mignerey[193], C. Palmer[193], C. Papageorgakis[193], M.M. Paranjpe[193], E. Popova[309,193], A. Shevelev[193], L. Zhang[193], C. Baldenegro Barrera[194], J. Bendavid[194], H. Bossi[194], S. Bright-Thonney[194], I.A. Cali[194], Y.c. Chen[194], P.c. Chou[194], M. D'Alfonso[194], J. Eysermans[194], C. Freer[194], G. Gomez-Ceballos[194], M. Goncharov[194], G. Grosso[194], P. Harris[194], D. Hoang[194], G.M. Innocenti[194], D. Kovalskyi[194], J. Krupa[194], L. Lavezzo[194], Y.-J. Lee[194], K. Long[194], C. Mcginn[194], A. Novak[194], M.I. Park[194], C. Paus[194], C. Reissel[194], C. Roland[194], G. Roland[194], S. Rothman[194], T.a. Sheng[194], G.S.F. Stephans[194], D. Walter[194], Z. Wang[194], B. Wyslouch[194], T. J. Yang[194], B. Crossman[195], W.J. Jackson[195], C. Kapsiak[195], M. Krohn[195], D. Mahon[195], J. Mans[195], B. Marzocchi[195], R. Rusack[195], O. Sancar[195], R. Saradhy[195], N. Strobbe[195], K. Bloom[196], D.R. Claes[196], G. Haza[196], J. Hossain[196], C. Joo[196], I. Kravchenko[196], A. Rohilla[196], J.E. Siado[196], W. Tabb[196], A. Vagnerini[196], A. Wightman[196], F. Yan[196], H. Bandyopadhyay[197], L. Hay[197], H.w. Hsia[197], I. Iashvili[197], A. Kalogeropoulos[197], A. Kharchilava[197], A. Mandal[197], M. Morris[197], D. Nguyen[197], S. Rappoccio[197], H. Rejeb Sfar[197], A. Williams[197], P. Young[197], D. Yu[197], G. Alverson[198], E. Barberis[198], J. Bonilla[198], B. Bylsma[198], M. Campana[198], J. Dervan[198], Y. Haddad[198], Y. Han[198], I. Israr[198], A. Krishna[198], M. Lu[198], N. Manganelli[198], R. Mccarthy[198],

D.M. Morse[198], T. Orimoto[198], A. Parker[198], L. Skinnari[198], C.S. Thoreson[198], E. Tsai[198], D. Wood[198], S. Dittmer[199], K.A. Hahn[199], Y. Liu[199], M. Mcginnis[199], Y. Miao[199], D.G. Monk[199], M.H. Schmitt[199], A. Taliercio[199], M. Velasco[199], J. Wang[199], G. Agarwal[200], R. Band[200], R. Bucci[200], S. Castells[200], A. Das[200], A. Ehnis[200], R. Goldouzian[200], M. Hildreth[200], K. Hurtado Anampa[200], T. Ivanov[200], C. Jessop[200], A. Karneyeu[200], K. Lannon[200], J. Lawrence[200], N. Loukas[200], L. Lutton[200], J. Mariano[200], N. Marinelli[200], I. Mcalister[200], T. McCauley[200], C. Mcgrady[200], C. Moore[200], Y. Musienko[240,200], H. Nelson[200], M. Osherson[200], A. Piccinelli[200], R. Ruchti[200], A. Townsend[200], Y. Wan[200], M. Wayne[200], H. Yockey[200], A. Basnet[201], M. Carrigan[201], R. De Los Santos[201], L.S. Durkin[201], C. Hill[201], M. Joyce[201], M. Nunez Ornelas[201], D.A. Wenzl[201], B.L. Winer[201], B. R. Yates[201], H. Bouchamaoui[202], K. Coldham[202], P. Das[202], G. Dezoort[202], P. Elmer[202], A. Frankenthal[202], M. Galli[202], B. Greenberg[202], N. Haubrich[202], K. Kennedy[202], G. Kopp[202], Y. Lai[202], D. Lange[202], A. Loeliger[202], D. Marlow[202], I. Ojalvo[202], J. Olsen[202], F. Simpson[202], D. Stickland[202], C. Tully[202], S. Malik[203], R. Sharma[203], A.S. Bakshi[204], S. Chandra[204], R. Chawla[204], A. Gu[204], L. Gutay[204], M. Jones[204], A.W. Jung[204], D. Kondratyev[204], M. Liu[204], M. Matthewman[204], G. Negro[204], N. Neumeister[204], G. Paspalaki[204], S. Piperov[204], J.F. Schulte[204], F. Wang[204], A. Wildridge[204], W. Xie[204], Y. Yao[204], Y. Zhong[204], N. Parashar[205], A. Pathak[205], E. Shumka[205], D. Acosta[206], A. Agrawal[206], C. Arbour[206], T. Carnahan[206], K.M. Ecklund[206], P.J. Fernández Manteca[206], S. Freed[206], P. Gardner[206], F.J.M. Geurts[206], T. Huang[206], I. Krommydas[206], N. Lewis[206], W. Li[206], J. Lin[206], O. Miguel Colin[206], B.P. Padley[206], R. Redjimi[206], J. Rotter[206], E. Yigitbasi[206], Y. Zhang[206], O. Bessidskaia Bylund[207], A. Bodek[207], P. de Barbaro[207,218], R. Demina[207], J.L. Dulemba[207], A. Garcia-Bellido[207], H.S. Hare[207], O. Hindrichs[207], N. Parmar[207], P. Parygin[309,207], H. Seo[207], R. Taus[207], B. Chiarito[208], J.P. Chou[208], S.V. Clark[208], S. Donnelly[208], D. Gadkari[208], Y. Gershtein[208], E. Halkiadakis[208], M. Heindl[208], C. Houghton[208], D. Jaroslawski[208], S. Konstantinou[208], I. Laflotte[208], A. Lath[208], J. Martins[208], B. Rand[208], J. Reichert[208], P. Saha[208], S. Salur[208], S. Schnetzer[208], S. Somalwar[208], R. Stone[208], S.A. Thayil[208], S. Thomas[208], J. Vora[208], D. Ally[209], A.G. Delannoy[209], S. Fiorendi[209], J. Harris[209], S. Higginbotham[209], T. Holmes[209], A.R. Kanuganti[209], N. Karunarathna[209], J. Lawless[209], L. Lee[209], E. Nibigira[209], B. Skipworth[209], S. Spanier[209], D. Aebi[210], M. Ahmad[210], T. Akhter[210], K. Androsov[210], A. Bolshov[210], O. Bouhali[310,210], R. Eusebi[210], P. Flanagan[210], J. Gilmore[210], Y. Guo[210], T. Kamon[210], S. Luo[210], R. Mueller[210], A. Safonov[210], N. Akchurin[211], J. Damgov[211], Y. Feng[211], N. Gogate[211], Y. Kazhykarim[211], K. Lamichhane[211], S.W. Lee[211], C. Madrid[211], A. Mankel[211], T. Peltola[211], I. Volobouev[211], E. Appelt[212], Y. Chen[212], S. Greene[212], A. Gurrola[212], W. Johns[212], R. Kunnawalkam Elayavalli[212], A. Melo[212], D. Rathjens[212], F. Romeo[212], P. Sheldon[212], S. Tuo[212], J. Velkovska[212], J. Viinikainen[212], J. Zhang[212], B. Cardwell[213], H. Chung[213], B. Cox[213], J. Hakala[213], R. Hirosky[213], M. Jose[213], A. Ledovskoy[213], C. Mantilla[213], C. Neu[213], C. RamónÁlvarez[213], S. Bhattacharya[214], P.E. Karchin[214], A. Aravind[215], S. Banerjee[215], K. Black[215], T. Bose[215], E. Chavez[215], S. Dasu[215], P. Everaerts[215], C. Galloni[215], H. He[215], M. Herndon[215], A. Herve[215], C.K. Koraka[215], S. Lomte[215], R. Loveless[215], A. Mallampalli[215], A. Mohammadi[215], S. Mondal[215], T. Nelson[215], G. Parida[215], L. Pétré[215], D. Pinna[215], A. Savin[215], V. Shang[215], V. Sharma[215], W.H. Smith[215], D. Teague[215], H.F. Tsoi[215], W. Vetens[215], A. Warden[215], S. Afanasiev[216], V. Alexakhin[216], Yu. Andreev[216], T. Aushev[216], D. Budkouski[216], R. Chistov[311,216], M. Danilov[311,216], T. Dimova[311,216], A. Ershov[311,216], S. Gninenko[216], I. Gorbunov[216], A. Gribushin[311,216], A. Kamenev[216], V. Karjavine[216], M. Kirsanov[216], V. Klyukhin[311,216], O. Kodolova[309,312,216], V. Korenkov[216], A. Kozyrev[311,216], N. Krasnikov[216], A. Lanev[216], A. Malakhov[216], V. Matveev[311,216], A. Nikitenko[312,313,216], V. Palichik[216], V. Perelygin[216], S. Petrushanko[311,216], S. Polikarpov[311,216], O. Radchenko[311,216], M. Savina[216], V. Shalaev[216], S. Shmatov[216], S. Shulha[216], Y. Skovpen[311,216], V. Smirnov[216], O. Teryaev[216], I. Tlisova[311,216], A. Toropin[216], N. Voytishin[216], B.S. Yuldashev[314,218,216], A. Zarubin[216], I. Zhizhin[216], E. Boos[217], V. Bunichev[217], M. Dubinin[302,217], V. Savrin[217], A. Snigirev[217], L. Dudko[217], K. Ivanov[217], V. Kim[240,217], V. Murzin[217], V. Oreshkin[217], D. Sosnov[217]

Collaboration Institutes

[1] Yerevan Physics Institute, Yerevan, Armenia
[2] Institut für Hochenergiephysik, Vienna, Austria
[3] Universiteit Antwerpen, Antwerpen, Belgium
[4] Vrije Universiteit Brussel, Brussel, Belgium
[5] Université Libre de Bruxelles, Bruxelles, Belgium
[6] Ghent University, Ghent, Belgium
[7] Université Catholique de Louvain, Louvain-la-Neuve, Belgium
[8] Centro Brasileiro de Pesquisas Fisicas, Rio de Janeiro, Brazil
[9] Universidade do Estado do Rio de Janeiro, Rio de Janeiro, Brazil
[10] Universidade Estadual Paulista, Universidade Federal do ABC, São Paulo, Brazil
[11] Institute for Nuclear Research and Nuclear Energy, Bulgarian Academy of Sciences, Sofia, Bulgaria
[12] University of Sofia, Sofia, Bulgaria
[13] Instituto De Alta Investigación, Universidad de Tarapacá, Casilla 7 D, Arica, Chile
[14] Universidad Tecnica Federico Santa Maria, Valparaiso, Chile
[15] Beihang University, Beijing, China
[16] Department of Physics, Tsinghua University, Beijing, China
[17] Institute of High Energy Physics, Beijing, China
[18] State Key Laboratory of Nuclear Physics and Technology, Peking University, Beijing, China
[19] State Key Laboratory of Nuclear Physics and Technology, Institute of Quantum Matter, South China Normal University, Guangzhou, China
[20] Sun Yat-Sen University, Guangzhou, China
[21] University of Science and Technology of China, Hefei, China
[22] Nanjing Normal University, Nanjing, China
[23] Institute of Modern Physics and Key Laboratory of Nuclear Physics and Ion-beam Application (MOE) - Fudan University, Shanghai, China
[24] Zhejiang University, Hangzhou, Zhejiang, China
[25] Universidad de Los Andes, Bogota, Colombia
[26] Universidad de Antioquia, Medellin, Colombia
[27] University of Split, Faculty of Electrical Engineering, Mechanical Engineering and Naval Architecture, Split, Croatia
[28] University of Split, Faculty of Science, Split, Croatia
[29] Institute Rudjer Boskovic, Zagreb, Croatia
[30] University of Cyprus, Nicosia, Cyprus
[31] Charles University, Prague, Czech Republic
[32] Escuela Politecnica Nacional, Quito, Ecuador
[33] Universidad San Francisco de Quito, Quito, Ecuador
[34] Academy of Scientific Research and Technology of the Arab Republic of Egypt, Egyptian Network of High Energy Physics, Cairo, Egypt
[35] Center for High Energy Physics (CHEP-FU), Fayoum University, El-Fayoum, Egypt
[36] National Institute of Chemical Physics and Biophysics, Tallinn, Estonia
[37] Department of Physics, University of Helsinki, Helsinki, Finland
[38] Helsinki Institute of Physics, Helsinki, Finland
[39] Lappeenranta-Lahti University of Technology, Lappeenranta, Finland
[40] IRFU, CEA, Université Paris-Saclay, Gif-sur-Yvette, France
[41] Laboratoire Leprince-Ringuet, CNRS/IN2P3, Ecole Polytechnique, Institut Polytechnique de Paris, Palaiseau, France
[42] Université de Strasbourg, CNRS, IPHC UMR 7178, Strasbourg, France

[43] Centre de Calcul de l'Institut National de Physique Nucleaire et de Physique des Particules, CNRS/IN2P3, Villeurbanne, France
[44] Institut de Physique des 2 Infinis de Lyon (IP2I), Villeurbanne, France
[45] Georgian Technical University, Tbilisi, Georgia
[46] RWTH Aachen University, I. Physikalisches Institut, Aachen, Germany
[47] RWTH Aachen University, III. Physikalisches Institut A, Aachen, Germany
[48] RWTH Aachen University, III. Physikalisches Institut B, Aachen, Germany
[49] Deutsches Elektronen-Synchrotron, Hamburg, Germany
[50] University of Hamburg, Hamburg, Germany
[51] Karlsruher Institut fuer Technologie, Karlsruhe, Germany
[52] Institute of Nuclear and Particle Physics (INPP), NCSR Demokritos, Aghia Paraskevi, Greece
[53] National and Kapodistrian University of Athens, Athens, Greece
[54] National Technical University of Athens, Athens, Greece
[55] University of Ioánnina, Ioánnina, Greece
[56] HUN-REN Wigner Research Centre for Physics, Budapest, Hungary
[57] MTA-ELTE Lendület CMS Particle and Nuclear Physics Group, Eötvös Loránd University, Budapest, Hungary
[58] Faculty of Informatics, University of Debrecen, Debrecen, Hungary
[59] HUN-REN ATOMKI - Institute of Nuclear Research, Debrecen, Hungary
[60] Karoly Robert Campus, MATE Institute of Technology, Gyongyos, Hungary
[61] Panjab University, Chandigarh, India
[62] University of Delhi, Delhi, India
[63] University of Hyderabad, Hyderabad, India
[64] Indian Institute of Technology Kanpur, Kanpur, India
[65] Saha Institute of Nuclear Physics, HBNI, Kolkata, India
[66] Indian Institute of Technology Madras, Madras, India
[67] IISER Mohali, India, Mohali, India
[68] Tata Institute of Fundamental Research-A, Mumbai, India
[69] Tata Institute of Fundamental Research-B, Mumbai, India
[70] National Institute of Science Education and Research, An OCC of Homi Bhabha National Institute, Bhubaneswar, Odisha, India
[71] Indian Institute of Science Education and Research (IISER), Pune, India
[72] Indian Institute of Technology Hyderabad, Telangana, India
[73] Isfahan University of Technology, Isfahan, Iran
[74] Institute for Research in Fundamental Sciences (IPM), Tehran, Iran
[75] University College Dublin, Dublin, Ireland
[76] INFN Sezione di Bari, Bari, Italy
[77] Università di Bari, Bari, Italy
[78] Politecnico di Bari, Bari, Italy
[79] INFN Sezione di Bologna, Bologna, Italy
[80] Università di Bologna, Bologna, Italy
[81] INFN Sezione di Catania, Catania, Italy
[82] Università di Catania, Catania, Italy
[83] INFN Sezione di Firenze, Firenze, Italy
[84] Università di Firenze, Firenze, Italy
[85] INFN Laboratori Nazionali di Frascati, Frascati, Italy
[86] INFN Sezione di Genova, Genova, Italy
[87] Università di Genova, Genova, Italy
[88] INFN Sezione di Milano-Bicocca, Milano, Italy
[89] Università di Milano-Bicocca, Milano, Italy
[90] INFN Sezione di Napoli, Napoli, Italy
[91] Università di Napoli 'Federico II', Napoli, Italy
[92] Università della Basilicata, Potenza, Italy
[93] Scuola Superiore Meridionale (SSM), Napoli, Italy
[94] INFN Sezione di Padova, Padova, Italy
[95] Università di Padova, Padova, Italy
[96] Universita degli Studi di Cagliari, Cagliari, Italy
[97] INFN Sezione di Pavia, Pavia, Italy
[98] Università di Pavia, Pavia, Italy
[99] INFN Sezione di Perugia, Perugia, Italy
[100] Università di Perugia, Perugia, Italy
[101] INFN Sezione di Pisa, Pisa, Italy
[102] Università di Pisa, Pisa, Italy
[103] Scuola Normale Superiore di Pisa, Pisa, Italy
[104] Università di Siena, Siena, Italy
[105] INFN Sezione di Roma, Roma, Italy
[106] Sapienza Università di Roma, Roma, Italy
[107] INFN Sezione di Torino, Torino, Italy
[108] Università di Torino, Torino, Italy
[109] Università del Piemonte Orientale, Novara, Italy
[110] INFN Sezione di Trieste, Trieste, Italy
[111] Università di Trieste, Trieste, Italy
[112] Kyungpook National University, Daegu, Korea
[113] Department of Mathematics and Physics - GWNU, Gangneung, Korea
[114] Chonnam National University, Institute for Universe and Elementary Particles, Kwangju, Korea
[115] Hanyang University, Seoul, Korea
[116] Korea University, Seoul, Korea
[117] Kyung Hee University, Department of Physics, Seoul, Korea
[118] Sejong University, Seoul, Korea
[119] Seoul National University, Seoul, Korea
[120] University of Seoul, Seoul, Korea
[121] Yonsei University, Department of Physics, Seoul, Korea
[122] Sungkyunkwan University, Suwon, Korea
[123] College of Engineering and Technology, American University of the Middle East (AUM), Dasman, Kuwait
[124] Kuwait University - College of Science - Department of Physics, Safat, Kuwait
[125] Riga Technical University, Riga, Latvia
[126] University of Latvia (LU), Riga, Latvia
[127] Vilnius University, Vilnius, Lithuania
[128] National Centre for Particle Physics, Universiti Malaya, Kuala Lumpur, Malaysia
[129] Universidad de Sonora (UNISON), Hermosillo, Mexico
[130] Centro de Investigacion y de Estudios Avanzados del IPN, Mexico City, Mexico
[131] Universidad Iberoamericana, Mexico City, Mexico
[132] Benemerita Universidad Autonoma de Puebla, Puebla, Mexico
[133] University of Montenegro, Podgorica, Montenegro
[134] University of Canterbury, Christchurch, New Zealand
[135] National Centre for Physics, Quaid-I-Azam University, Islamabad, Pakistan
[136] AGH University of Krakow, Krakow, Poland
[137] National Centre for Nuclear Research, Swierk, Poland
[138] Institute of Experimental Physics, Faculty of Physics, University of Warsaw, Warsaw, Poland
[139] Warsaw University of Technology, Warsaw, Poland
[140] Laboratório de Instrumentação e Física Experimental de Partículas, Lisboa, Portugal
[141] Faculty of Physics, University of Belgrade, Belgrade, Serbia
[142] VINCA Institute of Nuclear Sciences, University of Belgrade, Belgrade, Serbia
[143] Centro de Investigaciones Energéticas Medioambientales y Tecnológicas (CIEMAT), Madrid, Spain
[144] Universidad Autónoma de Madrid, Madrid, Spain
[145] Universidad de Oviedo, Instituto Universitario de Ciencias y Tecnologías Espaciales de Asturias (ICTEA), Oviedo, Spain
[146] Instituto de Física de Cantabria (IFCA), CSIC-Universidad de Cantabria, Santander, Spain
[147] University of Colombo, Colombo, Sri Lanka
[148] University of Ruhuna, Department of Physics, Matara, Sri Lanka
[149] CERN, European Organization for Nuclear Research, Geneva, Switzerland
[150] PSI Center for Neutron and Muon Sciences, Villigen, Switzerland

[151] ETH Zurich - Institute for Particle Physics and Astrophysics (IPA), Zurich, Switzerland
[152] Universität Zürich, Zurich, Switzerland
[153] National Central University, Chung-Li, Taiwan
[154] National Taiwan University (NTU), Taipei, Taiwan
[155] High Energy Physics Research Unit, Department of Physics, Faculty of Science, Chulalongkorn University, Bangkok, Thailand
[156] Tunis El Manar University, Tunis, Tunisia
[157] Çukurova University, Physics Department, Science and Art Faculty, Adana, Turkey
[158] Middle East Technical University, Physics Department, Ankara, Turkey
[159] Bogazici University, Istanbul, Turkey
[160] Istanbul Technical University, Istanbul, Turkey
[161] Istanbul University, Istanbul, Turkey
[162] Yildiz Technical University, Istanbul, Turkey
[163] Institute for Scintillation Materials of National Academy of Science of Ukraine, Kharkiv, Ukraine
[164] National Science Centre, Kharkiv Institute of Physics and Technology, Kharkiv, Ukraine
[165] University of Bristol, Bristol, United Kingdom
[166] Rutherford Appleton Laboratory, Didcot, United Kingdom
[167] Imperial College, London, United Kingdom
[168] Brunel University, Uxbridge, United Kingdom
[169] Baylor University, Waco, Texas, USA
[170] Bethel University, St. Paul, Minnesota, USA
[171] Catholic University of America, Washington, DC, USA
[172] The University of Alabama, Tuscaloosa, Alabama, USA
[173] Boston University, Boston, Massachusetts, USA
[174] Brown University, Providence, Rhode Island, USA
[175] University of California, Davis, Davis, California, USA
[176] University of California, Los Angeles, California, USA
[177] University of California, Riverside, Riverside, California, USA
[178] University of California, San Diego, La Jolla, California, USA
[179] University of California, Santa Barbara - Department of Physics, Santa Barbara, California, USA
[180] California Institute of Technology, Pasadena, California, USA
[181] Carnegie Mellon University, Pittsburgh, Pennsylvania, USA
[182] University of Colorado Boulder, Boulder, Colorado, USA
[183] Cornell University, Ithaca, New York, USA
[184] Fermi National Accelerator Laboratory, Batavia, Illinois, USA
[185] University of Florida, Gainesville, Florida, USA
[186] Florida State University, Tallahassee, Florida, USA
[187] Florida Institute of Technology, Melbourne, Florida, USA
[188] University of Illinois Chicago, Chicago, Illinois, USA
[189] The University of Iowa, Iowa City, Iowa, USA
[190] Johns Hopkins University, Baltimore, Maryland, USA
[191] The University of Kansas, Lawrence, Kansas, USA
[192] Kansas State University, Manhattan, Kansas, USA
[193] University of Maryland, College Park, Maryland, USA
[194] Massachusetts Institute of Technology, Cambridge, Massachusetts, USA
[195] University of Minnesota, Minneapolis, Minnesota, USA
[196] University of Nebraska-Lincoln, Lincoln, Nebraska, USA
[197] State University of New York at Buffalo, Buffalo, New York, USA
[198] Northeastern University, Boston, Massachusetts, USA
[199] Northwestern University, Evanston, Illinois, USA
[200] University of Notre Dame, Notre Dame, Indiana, USA
[201] The Ohio State University, Columbus, Ohio, USA
[202] Princeton University, Princeton, New Jersey, USA
[203] University of Puerto Rico, Mayaguez, Puerto Rico, USA
[204] Purdue University, West Lafayette, Indiana, USA
[205] Purdue University Northwest, Hammond, Indiana, USA
[206] Rice University, Houston, Texas, USA
[207] University of Rochester, Rochester, New York, USA
[208] Rutgers, The State University of New Jersey, Piscataway, New Jersey, USA
[209] University of Tennessee, Knoxville, Tennessee, USA
[210] Texas A&M University, College Station, Texas, USA
[211] Texas Tech University, Lubbock, Texas, USA
[212] Vanderbilt University, Nashville, Tennessee, USA
[213] University of Virginia, Charlottesville, Virginia, USA
[214] Wayne State University, Detroit, Michigan, USA
[215] University of Wisconsin - Madison, Madison, Wisconsin, USA
[216] Authors affiliated with an international laboratory covered by a cooperation agreement with CERN
[217] Authors affiliated with an institute formerly covered by a cooperation agreement with CERN
[218] Deceased
[219] Also at Yerevan State University, Yerevan, Armenia
[220] Also at TU Wien, Vienna, Austria
[221] Also at Ghent University, Ghent, Belgium
[222] Also at Universidade do Estado do Rio de Janeiro, Rio de Janeiro, Brazil
[223] Also at FACAMP - Faculdades de Campinas, Sao Paulo, Brazil
[224] Also at Universidade Estadual de Campinas, Campinas, Brazil
[225] Also at Federal University of Rio Grande do Sul, Porto Alegre, Brazil
[226] Also at The University of the State of Amazonas, Manaus, Brazil
[227] Also at University of Chinese Academy of Sciences, Beijing, China
[228] Also at China Center of Advanced Science and Technology, Beijing, China
[229] Now at Henan Normal University, Xinxiang, China
[230] Also at University of Shanghai for Science and Technology, Shanghai, China
[231] Now at The University of Iowa, Iowa City, Iowa, USA
[232] Also at Center for High Energy Physics, Peking University, Beijing, China
[233] Also at Cairo University, Cairo, Egypt
[234] Also at Suez University, Suez, Egypt
[235] Now at British University in Egypt, Cairo, Egypt
[236] Also at Purdue University, West Lafayette, Indiana, USA
[237] Also at Université de Haute Alsace, Mulhouse, France
[238] Also at Istinye University, Istanbul, Turkey
[239] Also at Tbilisi State University, Tbilisi, Georgia
[240] Also at an institute formerly covered by a cooperation agreement with CERN
[241] Also at University of Hamburg, Hamburg, Germany
[242] Also at RWTH Aachen University, III. Physikalisches Institut A, Aachen, Germany
[243] Also at Bergische University Wuppertal (BUW), Wuppertal, Germany
[244] Also at Brandenburg University of Technology, Cottbus, Germany
[245] Also at Forschungszentrum Jülich, Juelich, Germany
[246] Also at CERN, European Organization for Nuclear Research, Geneva, Switzerland
[247] Also at HUN-REN ATOMKI - Institute of Nuclear Research, Debrecen, Hungary
[248] Now at Universitatea Babes-Bolyai - Facultatea de Fizica, Cluj-Napoca, Romania
[249] Also at MTA-ELTE Lendület CMS Particle and Nuclear Physics Group, Eötvös Loránd University, Budapest, Hungary
[250] Also at HUN-REN Wigner Research Centre for Physics, Budapest, Hungary
[251] Also at Physics Department, Faculty of Science, Assiut University, Assiut, Egypt
[252] Also at The University of Kansas, Lawrence, Kansas, USA
[253] Also at Punjab Agricultural University, Ludhiana, India
[254] Also at University of Hyderabad, Hyderabad, India
[255] Also at Indian Institute of Science (IISc), Bangalore, India
[256] Also at University of Visva-Bharati, Santiniketan, India
[257] Also at IIT Bhubaneswar, Bhubaneswar, India
[258] Also at Institute of Physics, Bhubaneswar, India

[259] Also at Deutsches Elektronen-Synchrotron, Hamburg, Germany
[260] Also at Isfahan University of Technology, Isfahan, Iran
[261] Also at Sharif University of Technology, Tehran, Iran
[262] Also at Department of Physics, University of Science and Technology of Mazandaran, Behshahr, Iran
[263] Also at Department of Physics, Faculty of Science, Arak University, ARAK, Iran
[264] Also at Helwan University, Cairo, Egypt
[265] Also at Italian National Agency for New Technologies, Energy and Sustainable Economic Development, Bologna, Italy
[266] Also at Centro Siciliano di Fisica Nucleare e di Struttura Della Materia, Catania, Italy
[267] Also at Università degli Studi Guglielmo Marconi, Roma, Italy
[268] Also at Scuola Superiore Meridionale, Università di Napoli 'Federico II', Napoli, Italy
[269] Also at Fermi National Accelerator Laboratory, Batavia, Illinois, USA
[270] Also at Lulea University of Technology, Lulea, Sweden
[271] Also at Consiglio Nazionale delle Ricerche - Istituto Officina dei Materiali, Perugia, Italy
[272] Also at UPES - University of Petroleum and Energy Studies, Dehradun, India
[273] Also at Institut de Physique des 2 Infinis de Lyon (IP2I), Villeurbanne, France
[274] Also at Department of Applied Physics, Faculty of Science and Technology, Universiti Kebangsaan Malaysia, Bangi, Malaysia
[275] Also at Trincomalee Campus, Eastern University, Sri Lanka, Nilaveli, Sri Lanka
[276] Also at Saegis Campus, Nugegoda, Sri Lanka
[277] Also at National and Kapodistrian University of Athens, Athens, Greece
[278] Also at Ecole Polytechnique Fédérale Lausanne, Lausanne, Switzerland
[279] Also at Universität Zürich, Zurich, Switzerland
[280] Also at Stefan Meyer Institute for Subatomic Physics, Vienna, Austria
[281] Also at Near East University, Research Center of Experimental Health Science, Mersin, Turkey
[282] Also at Konya Technical University, Konya, Turkey
[283] Also at Izmir Bakircay University, Izmir, Turkey
[284] Also at Adiyaman University, Adiyaman, Turkey
[285] Also at Bozok Universitetesi Rektörlügü, Yozgat, Turkey
[286] Also at Istanbul Sabahattin Zaim University, Istanbul, Turkey
[287] Also at Marmara University, Istanbul, Turkey
[288] Also at Milli Savunma University, Istanbul, Turkey
[289] Also at Informatics and Information Security Research Center, Gebze/Kocaeli, Turkey
[290] Also at Kafkas University, Kars, Turkey
[291] Now at Istanbul Okan University, Istanbul, Turkey
[292] Also at Hacettepe University, Ankara, Turkey
[293] Also at Erzincan Binali Yildirim University, Erzincan, Turkey
[294] Also at Istanbul University - Cerrahpasa, Faculty of Engineering, Istanbul, Turkey
[295] Also at Yildiz Technical University, Istanbul, Turkey
[296] Also at School of Physics and Astronomy, University of Southampton, Southampton, United Kingdom
[297] Also at Monash University, Faculty of Science, Clayton, Australia
[298] Also at Bethel University, St. Paul, Minnesota, USA
[299] Also at Università di Torino, Torino, Italy
[300] Also at Karamanoğlu Mehmetbey University, Karaman, Turkey
[301] Also at California Lutheran University;, Thousand Oaks, California, USA
[302] Also at California Institute of Technology, Pasadena, California, USA
[303] Also at United States Naval Academy, Annapolis, Maryland, USA
[304] Also at Bingol University, Bingol, Turkey
[305] Also at Georgian Technical University, Tbilisi, Georgia
[306] Also at Sinop University, Sinop, Turkey
[307] Also at Erciyes University, Kayseri, Turkey
[308] Also at Horia Hulubei National Institute of Physics and Nuclear Engineering (IFIN-HH), Bucharest, Romania
[309] Now at another institute formerly covered by a cooperation agreement with CERN
[310] Also at Hamad Bin Khalifa University (HBKU), Doha, Qatar
[311] Also at another institute formerly covered by a cooperation agreement with CERN
[312] Also at Yerevan Physics Institute, Yerevan, Armenia
[313] Also at Imperial College, London, United Kingdom
[314] Also at Institute of Nuclear Physics of the Uzbekistan Academy of Sciences, Tashkent, Uzbekistan

References

[1] I. Arsene, et al., BRAHMS, Quark gluon plasma and color glass condensate at RHIC? the perspective from the BRAHMS experiment, Nucl. Phys. A 757 (2005) 1. arXiv eprint arXiv:0410020, https://doi.org/10.1016/j.nuclphysa.2005.02.130
[2] CMS Collaboration, Overview of high-density QCD studies with the CMS experiment at the LHC, Phys. Rept. (2025). https://doi.org/10.48550/arXiv.2405.10785
[3] J.-Y. Ollitrault, Anisotropy as a signature of transverse collective flow, Phys. Rev. D 46 (1992) 229. https://doi.org/10.1103/PhysRevD.46.229
[4] S. Voloshin, Y. Zhang, Flow study in relativistic nuclear collisions by fourier expansion of azimuthal particle distributions, Z. Phys. C 70 (1996) 665. arXiv eprint arXiv:9407282, https://doi.org/10.1007/s002880050141
[5] CMS Collaboration, Observation of correlated azimuthal anisotropy fourier harmonics in pp and p + Pb collisions at the LHC, Phys. Rev. Lett. 120 (2018) 092301. arXiv eprint arXiv:1709.09189, https://doi.org/10.1103/PhysRevLett.120.092301
[6] ALICE Collaboration, Investigations of anisotropic flow using multiparticle azimuthal correlations in pp, p-Pb, Xe-Xe, and Pb-Pb collisions at the LHC, Phys. Rev. Lett. 123 (2019) 142301. arXiv eprint arXiv:1903.01790, https://doi.org/10.1103/PhysRevLett.123.142301
[7] J. Noronha-Hostler, L. Yan, F.G. Gardim, J.-Y. Ollitrault, Linear and cubic response to the initial eccentricity in heavy-ion collisions, Phys. Rev. C 93 (2016) 014909. arXiv eprint arXiv:1511.03896, https://doi.org/10.1103/PhysRevC.93.014909
[8] M. Bender, P.-H. Heenen, P.-G. Reinhard, Self-consistent mean-field models for nuclear structure, Rev. Mod. Phys. 75 (2003) 121. https://doi.org/10.1103/RevModPhys.75.121
[9] B. Bally, M. Bender, G. Giacalone, V. Somà, Evidence of the triaxial structure of ^{129}Xe at the large hadron collider, Phys. Rev. Lett. 128 (2022) 082301. arXiv eprint arXiv:2108.09578, https://doi.org/10.1103/PhysRevLett.128.082301
[10] J. Jia, Shape of atomic nuclei in heavy ion collisions, Phys. Rev. C 105 (2022) 014905. arXiv eprint arXiv:2106.08768, https://doi.org/10.1103/PhysRevC.105.014905
[11] CMS Collaboration, Precision luminosity measurement in proton-proton collisions at $\sqrt{s} = 13$ TeV in 2015 and 2016 at CMS, Eur. Phys. J. C 81 (2021) 800. arXiv eprint arXiv:2104.01927, https://doi.org/10.1140/epjc/s10052-021-09538-2
[12] CMS Collaboration, CMS luminosity measurement using 2017 proton-proton collisions at $\sqrt{s} = 13$ TeV, 2018. CMS Physics Analysis Summary CMS-PAS-LUM-17-004, 2018, http://cds.cern.ch/record/2628652,
[13] CMS Collaboration, CMS Luminosity Measurement Using Nucleus–Nucleus Collisions at $\sqrt{s_{NN}} = 5.02$ TeV in 2018, CMS Physics Analysis Summary, 2022. https://cds.cern.ch/record/2809613,
[14] 2025, (HEPData record for this analysis). https://doi.org/10.17182/hepdata.161536
[15] CMS Collaboration, Description and performance of track and primary-vertex reconstruction with the CMS tracker, JINST 9 (2014) P10009. arXiv eprint arXiv:1405.6569, https://doi.org/10.1088/1748-0221/9/10/P10009
[16] CMS Collaboration, The CMS experiment at the CERN LHC, JINST 3 (2008) S08004. https://doi.org/10.1088/1748-0221/3/08/S08004
[17] S. Agostinelli, et al., GEANT4, GEANT4—a simulation toolkit, Nucl. Instrum. Meth. A 506 (2003) 250. https://doi.org/10.1016/S0168-9002(03)01368-8
[18] CMS Collaboration, Charged-particle angular correlations in XeXe collisions at $\sqrt{s_{NN}} = 5.44$ TeV, Phys. Rev. C 100 (2019) 044902. arXiv eprint arXiv:1901.07997, https://doi.org/10.1103/PhysRevC.100.044902
[19] CMS Collaboration, The CMS trigger system, JINST 12 (2017) P01020. arXiv eprint arXiv:1609.02366, https://doi.org/10.1088/1748-0221/12/01/P01020
[20] CMS Collaboration, A DNN for CMS track classification and selection, EPJ Web Conf. 295 (2024) 03001. arXiv eprint arXiv:2311.05157, https://doi.org/10.1051/epjconf/202429503001
[21] CMS Collaboration, Measurement of the pseudorapidity and centrality dependence of the transverse energy density in PbPb collisions at $\sqrt{s_{NN}} = 2.76$ TeV, Phys. Rev. Lett. 109 (2012) 152303. arXiv eprint arXiv:1205.2488, https://doi.org/10.1103/PhysRevLett.109.152303
[22] ALICE Collaboration, Measurements of mixed harmonic cumulants in Pb–Pb collisions at $\sqrt{s_{NN}} = 5.02$ TeV, Phys. Lett. B 818 (2021) 136354. arXiv eprint arXiv:2102.12180, https://doi.org/10.1016/j.physletb.2021.136354
[23] CMS Collaboration, Evidence for collectivity in pp collisions at the LHC, Phys. Lett. B 765 (2017) 193. arXiv eprint arXiv:1606.06198, https://doi.org/10.1016/j.physletb.2016.12.009
[24] A. Bilandzic, R. Snellings, S. Voloshin, Flow analysis with cumulants: direct calculations, Phys. Rev. C 83 (2011) 044913. arXiv eprint arXiv:1010.0233, https://doi.org/10.1103/PhysRevC.83.044913

[25] A. Bilandzic, C.H. Christensen, K. Gulbrandsen, A. Hansen, Y. Zhou, Generic framework for anisotropic flow analyses with multiparticle azimuthal correlations, Phys. Rev. C 89 (2014) 064904. arXiv eprint arXiv:1312.3572, https://doi.org/10.1103/PhysRevC.89.064904

[26] ALICE Collaboration, Correlated event-by-event fluctuations of flow harmonics in Pb-Pb collisions at $\sqrt{s_{\rm NN}} = 2.76$ TeV, Phys. Rev. Lett. 117 (2016) 182301. arXiv eprint arXiv:1604.07663, https://doi.org/10.1103/PhysRevLett.117.182301

[27] C. Mordasini, A. Bilandzic, D. Karakoç, S.F. Taghavi, Higher order symmetric cumulants, Phys. Rev. C 102 (2020) 024907. arXiv eprint arXiv:1901.06968, https://doi.org/10.1103/PhysRevC.102.024907

[28] Z. Moravcova, K. Gulbrandsen, Y. Zhou, Generic algorithm for multiparticle cumulants of azimuthal correlations in high energy nucleus collisions, Phys. Rev. C 103 (2021) 024913. arXiv eprint arXiv:2005.07974, https://doi.org/10.1103/PhysRevC.103.024913

[29] I.P. Lokhtin, A.M. Snigirev, A model of jet quenching in ultrarelativistic heavy ion collisions and high-p_T hadron spectra at RHIC, Eur. Phys. J. C 45 (2006) 211. arXiv eprint arXiv:0506189, https://doi.org/10.1140/epjc/s2005-02426-3

[30] B. Schenke, P. Tribedy, R. Venugopalan, Fluctuating glasma initial conditions and flow in heavy ion collisions, Phys. Rev. Lett. 108 (2012) 252301. arXiv eprint arXiv:1202.6646, https://doi.org/10.1103/PhysRevLett.108.252301

[31] S. McDonald, C. Shen, F. Fillion-Gourdeau, S. Jeon, C. Gale, A detailed study and synthesis of flow observables in the IP-Glasma + MUSIC + UrQMD framework, Nucl. Phys. A 967 (2017) 393. arXiv eprint arXiv:1704.05362, https://doi.org/10.1016/j.nuclphysa.2017.05.053

[32] C. Gale, S. Jeon, B. Schenke, Hydrodynamic modeling of heavy-ion collisions, Int. J. Mod. Phys. A 28 (2013) 1340011. arXiv eprint arXiv:1301.5893, https://doi.org/10.1142/S0217751X13400113

[33] S.A. Bass, et al., Microscopic models for ultrarelativistic heavy ion collisions, Prog. Part. Nucl. Phys. 41 (1998) 255. arXiv eprint arXiv:9803035, https://doi.org/10.1016/S0146-6410(98)00058-1

[34] B. Schenke, C. Shen, P. Tribedy, Running the gamut of high energy nuclear collisions, Phys. Rev. C 102 (4) (2020) 044905. arXiv eprint arXiv:2005.14682, https://doi.org/10.1103/PhysRevC.102.044905

[35] J.S. Moreland, J.E. Bernhard, S.A. Bass, Alternative ansatz to wounded nucleon and binary collision scaling in high-energy nuclear collisions, Phys. Rev. C 92 (2015) 011901. arXiv eprint arXiv:1412.4708, https://doi.org/10.1103/PhysRevC.92.011901

[36] G. Giacalone, J. Noronha-Hostler, M. Luzum, J.-Y. Ollitrault, Hydrodynamic predictions for 5.44 TeV Xe + Xe collisions, Phys. Rev. C 97 (2018) 034904. arXiv eprint arXiv:1711.08499, https://doi.org/10.1103/PhysRevC.97.034904

[37] F.G. Gardim, F. Grassi, M. Luzum, J.-Y. Ollitrault, Mapping the hydrodynamic response to the initial geometry in heavy-ion collisions, Phys. Rev. C 85 (2012) 024908. arXiv eprint arXiv:1111.6538, https://doi.org/10.1103/PhysRevC.85.024908

[38] H. Mäntysaari, B. Schenke, C. Shen, W. Zhao, Probing nuclear structure of heavy ions at energies available at the CERN large hadron collider, Phys. Rev. C 110 (2024) 054913. arXiv eprint arXiv:2409.19064, https://doi.org/10.1103/PhysRevC.110.054913

[39] S. Zhao, H.-j. Xu, Y. Zhou, Y.-X. Liu, H. Song, Exploring the nuclear shape phase transition in ultra-relativistic ^{129}Xe + ^{129} Xe collisions at the LHC, Phys. Rev. Lett. 133 (2024) 192301. arXiv eprint arXiv:2403.07441, https://doi.org/10.1103/PhysRevLett.133.192301

[40] K. Werner, Core-corona separation in ultrarelativistic heavy ion collisions, Phys. Rev. Lett. 98 (2007) 152301. arXiv eprint arXiv:0704.1270, https://doi.org/10.1103/PhysRevLett.98.152301

[41] K. Werner, B. Guiot, I. Karpenko, T. Pierog, Analysing radial flow features in p-Pb and p-p collisions at several TeV by studying identified particle production in EPOS3, Phys. Rev. C 89 (6) (2014) 064903. arXiv eprint arXiv:1312.1233, https://doi.org/10.1103/PhysRevC.89.064903

[42] ALICE Collaboration, Multiharmonic correlations of different flow amplitudes in Pb-Pb collisions at $\sqrt{s_{\rm NN}} = 2.76$ TeV, Phys. Rev. Lett. 127 (2021) 092302. arXiv eprint arXiv:2101.02579, https://doi.org/10.1103/PhysRevLett.127.092302

[43] W. Zhao, H.-j. Xu, H. Song, Collective flow in 2.76 a TeV and 5.02 a TeV Pb + Pb collisions, Eur. Phys. J. C 77 (2017) 645. arXiv eprint arXiv:1703.10792, https://doi.org/10.1140/epjc/s10052-017-5186-x